Effect of Fiber Morphology on Tensile Properties of Polypropylene Cement Composites

by

Himai Ashok Mehere

A Thesis Presented in Partial Fulfillment
of the Requirements for the Degree
Master of Science

Approved April 2017 by the
Graduate Supervisory Committee:

Barzin Mobasher, Chair
Subramaniam Dharmarajan
Narayanan Neithalath

ARIZONA STATE UNIVERSITY

May 2017

ABSTRACT

The main objective of this study is to investigate the effect of polypropylene fiber morphology on the tensile response of cementitious composites. Two proprietary polypropylene fibers manufactured by BASF – MAC 2200CB, a crimped monofilament macro fiber and MF40, a bundled multi filament polypropylene made up of 500 filaments,40-micron diameter each were compared. The stiff structure and crimped geometry of MAC 2200 CB was studied in comparison with the multifilament MF40, which provide a higher surface area and a bundled fiber effect. Uniaxial tensile tests were performed on individual fibers to study fiber strength and failure pattern at three different gage lengths. The interaction of these 2 fibers with cement matrix was studied under varying strain rate, embedded fiber length and matrix mixes by a series of quassi - static fiber pullout tests. Unidirectional filament wound composite laminates were manufactures with the two fibers and only MF40 woven textiles were used to manufacture MF40 textile reinforced composites. The mechanical behavior of polypropylene fiber and textile reinforced cementitious composites subjected to static tensile loading with the effects of fiber type and dosage, textile weave and dosage, matrix formulations, processing techniques etc. is studied. Evolution of distributed cracking mechanism and local strain fields was documented using digital image correlation (DIC) and correlated with the tensile response and stiffness degradation. VIC 3D-7, commercial software developed by Correlated Solutions, Inc. was used to run the DIC analysis for the tensile tests on laminates. The DIC technique was further used for automated determination of crack density, crack spacing, and characterizing damage evolution.

To my parents,

I am nothing without you.

ACKNOWLEDGMENTS

Foremost, I would like to express my sincere gratitude to my advisor Dr. Barzin Mobasher for the continuous support of my research, for his patience, motivation, enthusiasm, and immense knowledge. His guidance helped me in all the time of research and writing of this thesis. I also want to extend my appreciation to Dr. Subramaniam D. Rajan and Dr. Narayanan Neithalath who served as my committee members, helping and supervising my progress in Master's degree program.

I would also like to thank Dr. Yiming Yao and Dr. Vikram Dey who taught me almost every basic skill including preparing and conducting experiment, data analysis. Dr. Yiming Yao's mentorship helped me gauge many complex ideas which he simplified for me paving a straightforward path for my work. I would like to sincerely thank Jacob Bauchmoyer, Dafnik Saril Kumar and Vinodh Vijayasarthy for their immense help in all the experimental work under my project. I also appreciate the assistance provided by Mr. Peter Goguen and Mr. Jeff Long for all their help in the laboratory.

Thanks to my dear friends Ankita Premi,Yogesh Unde, and Megha Gohel, for always helping me out. I extend my heartfelt gratitude to my boyfriend, Supal Bhosale for his love and appreciation; my friends – Anagha Phusate, Kalyani Poharkar, Awani Nimbarte, and Neha Wanare for providing me with the moral support on days of distress and also my family members - Rahul, Twinkle and my dear grandmother for her words of wisdom.

Lastly, I would like to thank my mother, Bhuneshwari Mehere and my father, Ashok Mehere for bringing me in this world. Their relentless efforts, constant support and unshakable faith in me, has helped me achieve everything in my master's journey.

TABLE OF CONTENTS

CHAPTER Page

CHAPTER Page

CHAPTER Page

LIST OF TABLES

Table Page

LIST OF FIGURES

Figure Page

Figure Page

Figure Page

Figure Page

1.INTRODUCTION TO POLYPROPYLENE REINFORCED CEMENT COMPOSITES

1.1 Introduction

Use of concrete as a structural material is limited in applications where superior tensile, flexural and impact resistance is required**.** Although it offers many advantages like high compressive strength, fire resistance and economic construction, the brittle behavior of the material remains a major issue for seismic and other applications where flexible behavior is essentially required. This shortcoming can be overcome by use of fibers as reinforcement which improves the mechanical response of concrete by providing a toughening mechanism and crack bridging.

Tremendous research has been conducted in the field of fiber reinforced concrete since the 1970's which has helped understand the fundamentals behind such complex composite behavior. The work of Aveston et al. (1971) [1], (1973) [2], Laws [3](1971), Stang and Shah [4](1986) etc. laid the foundation for study of composite behavior, enabling engineers all over the world to use composite technology to its potential application. In the last 40 -50 years, there has been marginal improvement in understanding and application of composites in aerospace, construction, textile and material industries. Steel FRC is widely used in structures under bending. FRC slabs used at London Heathrow Airport parking and foundation of Postdamer platz in Berlin [5] have been the early applications.

Fiber and textile reinforced composites are part of the general class of engineering materials called composites. Composites are characterized by being multiphase materials within which the phase distribution and the geometry can be tailored to optimize one or more properties. There are several forms of composites based on the fiber type, material,

matrix type and processing techniques and each one has varied applications. Numerous materials choices can be used with a range of manufacturing techniques.

These composites can be broadly classified as continuous fiber and discontinuous or short fiber reinforced systems. Examples of continuous fiber reinforcement includes unidirectional, woven cloth and helical winding. These are made into laminates by stacking a single ply – continuous reinforced layer into different orientations throughout the thickness of the composite. Alignment of short dispersed fibers can be carried out by hydrodynamic methods of alignment in the tension direction Short fibers however, are mostly dispersed and randomly oriented in the matrix. Continuous fiber reinforced systems can be classified as "advanced composites," which make use of the advanced fibers and their orientation, advanced matrices and processing techniques. Figure 1 shows a broad classification of fiber reinforcement.

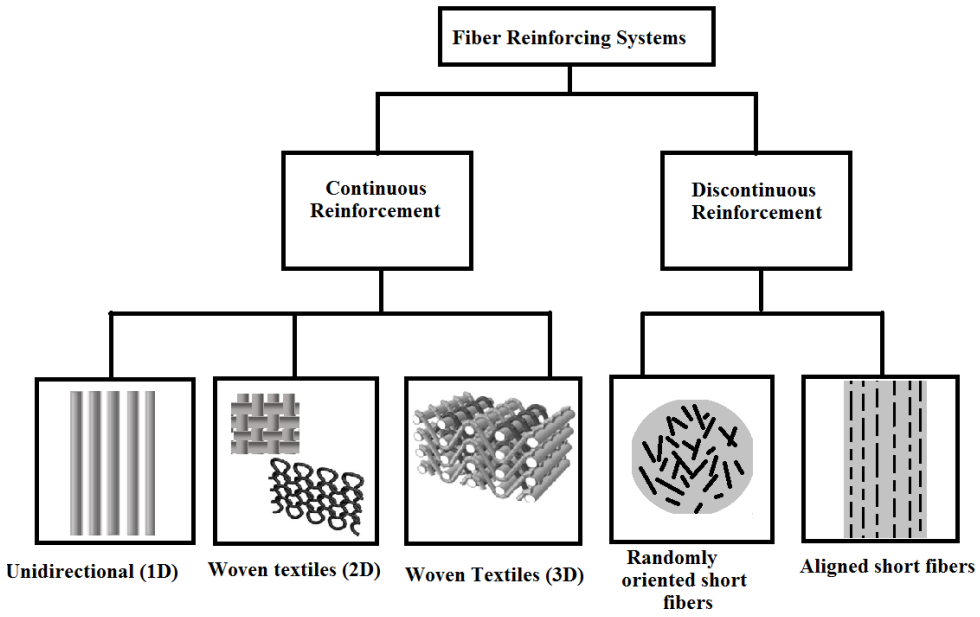

Figure 1. Classification of fiber reinforcing systems.
(2D and 3D textile schematic from Journal of Industrial Textiles [6])

Unidirectional laminated composites exhibit excellent in-plane but poor inter-laminar properties. This is due to lack of reinforcements in the thickness direction and leads to poor damage tolerance in the presence of inter-laminar stresses. Plain weave fabrics are used as reinforcements in composites to obtain balanced ply properties and improved inter-laminar properties. In textile, reinforced composites, the fibers used are first conformed into the shape of a textile. Despite the reduced stiffness and strength in the in-plane directions, fabrics are advantageous because of improved cost of manufacturing. It is therefore important to study the mechanical behavior of such composites to fully realize their potential. This study revolves around the use of polypropylene fibers in composites with 1D and 2D reinforcement and its study from a life scale to full scale optimized lightweight structural shapes which provide the strength of concrete and toughness and crack resistance of the reinforcing fibers

1.1.1 Polypropylene

Polypropylene fibers are thermoplastic polymers derived from monomeric C3H6 which is purely a hydrocarbon. It is the world's second most widely produced synthetic plastic. About 4 million tons of polypropylene fibers are produced in the world every year for various applications in synthetics, packaging, textile, chemical solvents and automobile component industries. Polypropylene fibers provide high alkaline and acid resistance. They are highly crystalline, stiff and exhibit good resistance to chemical and bacterial attack. High molecular weight makes it useful for various applications. Monofilament polypropylene fibers can be used in much lower content than steel fibers. The tensile strength and other mechanical properties are enhanced by subsequent multi stage drawing. Polypropylene fibers are also compatible with all concrete chemical admixtures. The

hydrophobic surface of fibers not being wet by cement paste, helps to prevent balling effect by chopped fibers. Presence of fibers reduces the settlement and bleeding in concrete [7]. Due to the ease in manufacturing, low cost and homogenous and consistent make, they are the most popular synthetic fibers used in the construction industry as secondary reinforcement. Use of these fibers reduces safety hazards, labor and placement costs and corrosion compared to conventional wire meshing.

1.1.2 Development of Polypropylene Reinforced Cement Composites

Polypropylene fibers were first suggested for use in 1965 as an admixture in concrete for construction of blast resistant buildings meant for the US Corps of Engineers. Investigations on use of polypropylene in concrete was first studied by Shell Chemicals Co. [8]. Hannat et al. [9] showed that inclusion of continuous fibrillated polypropylene films in cement mortar enhances the load carrying capacity of continuous polypropylene reinforced cement sheets. Applications included cladding, flat and corrugated sheeting, cavity panels, underwater pipes, thin shell concrete roofing materials etc. Such various non-load bearing structural members which required impact resistance were studied with impact resistance and durability in view. Closely spaced multiple crack formation was studied in the future decades. Numerous studies in different types of fibers reinforced in concrete were undertaken and their behavior was studied with respect to improving strength, toughness, durability, impact and fatigue resistance. Studies with polypropylene reinforcement showed increase in post crack energy absorption capacity and ductility, flexural fatigue strength and the endurance limit. [10]; improved impact resistance and flexural behavior [11]. Analytical relationships were proposed to predict the stress-strain responses and toughness index of the composite was derived [12]. Damage characteristics

in such systems were studied by Stang et al. [13] where relationship between specific crack surface and strain was used to document damage evolution for PP FRC. Mobasher [14] used image analysis of cement composites of different volume fractions of polypropylene using crack density, length and spacing as damage parameters.

1.1.3 Project Overview

Two proprietary polypropylene fibers manufactured by BASF Corporation for use in textile reinforced concrete were studied. Surface modified MAC 2200CB, a crimped monofilament macro fiber and MF40, a bundled multi filament polypropylene made up of 500 filaments,40-micron diameter each were compared. The stiff structure and crimped geometry of MAC 2200 CB was studied in comparison with the multifilament MF40, which provide a higher surface area and a bundled fiber effect. MAC 2200CB is a chemically modified master fiber developed by BASF which can be used in applications such as cast in place precast concrete slabs, bridge decks, concrete pavements etc. It can also serve as temperature and shrinkage reinforcement. The crimped geometry and chemically enhanced surface provides superior bonding to cementitious matrices, thus increasing the post crack load-carrying capacity and toughness of fiber reinforced concrete [15]. To evaluate the performance of these polymeric fibers individually, uniaxial tests were performed to understand their tensile strength, toughness and strain sensitivity.

A novel polymer resin technology was used to manufacture the fiber which chemically enhances the fiber bond with the cement matrix leading to hydration products bonded to the fiber structure. Hence, the fiber name is suffixed with CB which stands for the chemical bond it provides with the cementitious matrix. MF40 however, is a recently developed straight multifilament bundled fiber. Various studies on behavior of bundles

fiber have been conducted to understand the bundled strength, bond characteristic and stress transfer of such systems.

Figure 2 shows the SEM images of MAC and bundled MF40 Figure 2 (c) and (d) show the textiles manufactured in open and tricot weave fashion using MF40.

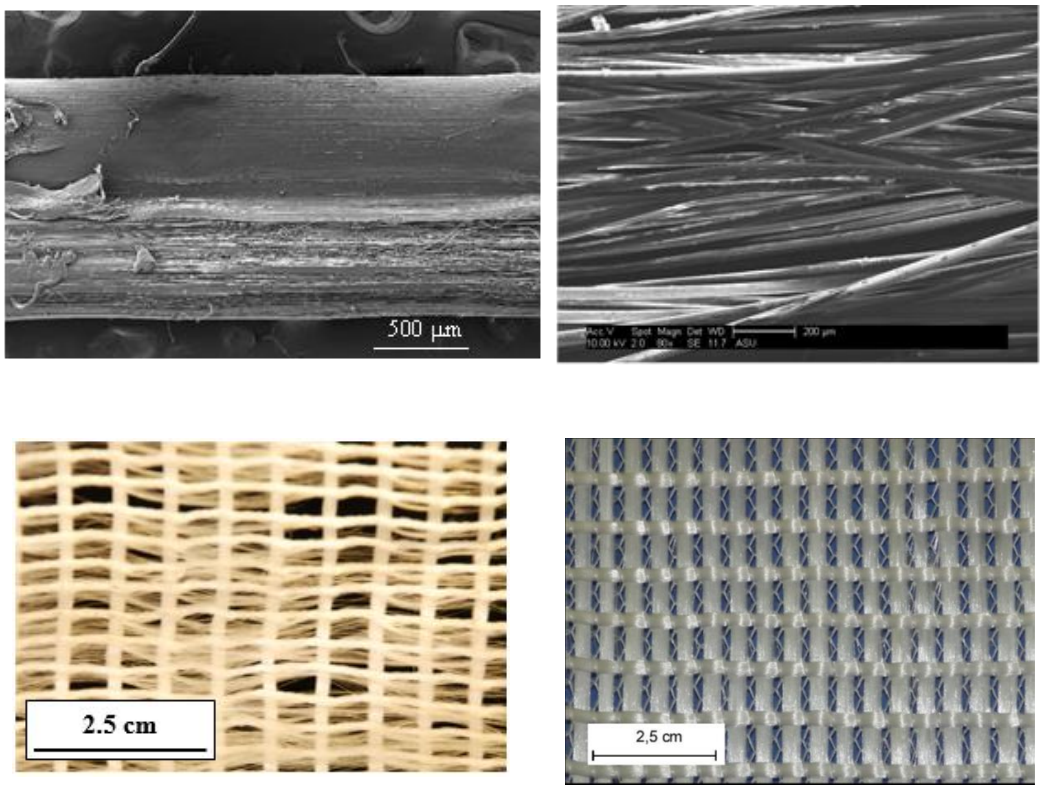

Figure 2. (a) Macro-synthetic MAC 2200CB fiber, (b) multifilament fibrillated microfiber (c) open weave MF40 textile (d) Tricot weave MF40 textile

Tensile tests were conducted on both unidirectional and textile reinforced coupons. Stress strain response was evaluated to study the cracking strengths, multiple cracking and ultimate strength and toughness parameters for varying fiber content, fiber types and matrix modifications. Full scale pultruded structural shapes were studied to understand their ability to be used as light gage structural members. Multiple cracking was documented using digital image correlation for the shapes.

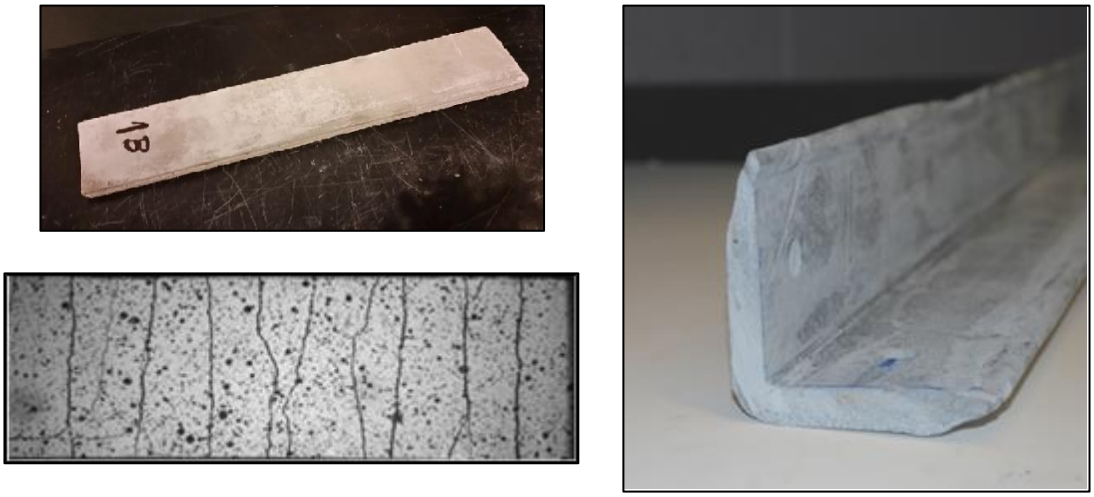

Figure 3. (a) Finished and cured unidirectional MAC 4% laminate, (b) Multiple cracking for a tested MAC 4% sample (c) Pultruded TRC channel section.

1.1.4 Fiber and Matrix Interface Characterization

The interfacial bond between the polymeric fibers and hydrating cement based matrix has always been one of the main drawbacks in the application development. Low bond strength does not allow effective force transfer between fiber and the matrix due to the weak nature of organic-inorganic bond. Enhanced composite behavior is primarily governed by this interfacial bond characteristic between fiber and matrix. Matrix interface plays a very important role in controlling mechanical properties of cementitious composites. Bond characteristics of fiber-cement systems using analytical and experimental techniques have shown to be the most significant parameter that characterizes the interface parameters and toughening mechanisms [16,17]. Peled et al reported that the bond is highly dependent on geometry of the fabric and its geometry. [18]. The modulus of elasticity of the yarns as well as the geometry of the reinforcing yarns contributes to the pullout behavior and bonding of the various systems. [19]. This calls for a detailed study

of fiber matrix interaction for monofilament MAC and MF40 microfiber bundle, before we can compare their composite response.

Interfacial bond characteristics can be quantified by performing fiber pullout tests. An experimental and analytical investigation was performed to measure the pull-out resistance of fibers from blended cement matrices. The effect of curing age, fiber embedded length, fiber and matrix types on the fiber-matrix interface and rate sensitivity were studied. A series of samples were prepared based on combinations of fiber type, fabric embedded length EL, mixture type and crosshead displacement rate of pullout. Figure shows the fully prepared and cured pullout specimen and (b) specimen structure from within for an un-bonded MF40 specimen. Behavior of these fibers with matrix is thus studied in detail.

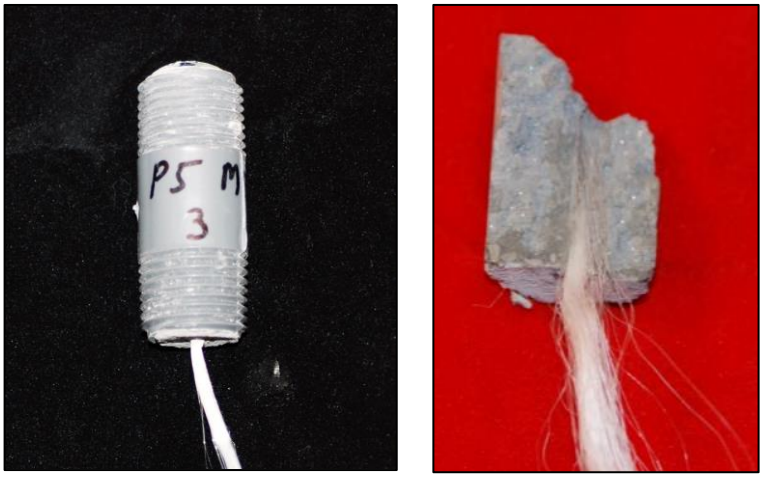

Figure 4. (a) MF40 Pullout Specimen, (b) internal structure of MF40 bonded with cement matrix.

1.1.5 Digital Image Correlation Technique

Digital Image Correlation has been a widely accepted, reliable and robust, non-contacting method of measuring deformation in the field of experimental mechanics. It is an optical measurement system which tracks the deformation of a planar region over a

period and correlates the deformations to characterize strains. Quantitative deformation measurement was limited due to constraints on contacting instruments like extensometers, clip gages due to specimen sizes, region of interest, mounting issues etc. To address these issues, optical deformation measurement proves to be a powerful tool which provides an accuracy in strain measurement ranging from a few micro strains to point by point smoothened strain response. It can be applicable to a wide range of specimen sizes and can map 2D and 3 D specimen response.

The field of optical measurement saw a breakthrough in the 1980's with development of high speed imaging techniques, robust computational systems which employed correlation algorithms which was the invention of digital image correlation. In the 1960's with the invention of lasers, interferometry etc. full field measurement of materials became popular. Displacement measurement by speckled photography introduced the concept of full scale deformation measurement using grids [20]. An optimized digital correlation method (DCM) was developed by Chu et al, [21] in 1986 using simple coarse-fine iterative techniques. This formed the basis of experimental testing with DIC. In recent years, Yao et al [22] used DIC for damage evaluation of TRC response at high strain rates. The applicability of DIC as a technique in terms of scale, range and reliability has been quite powerful compared to conventional contacting deformation measurement systems.

In this study, image analysis by means of three-dimensional digital image correlation (DIC) method was used to quantify the non-uniform displacement and strain distributions. Distributed cracking mechanism was quantified by measuring damage parameters namely, crack width and spacing. Figure shows the DIC displacement field for

MAC 4% laminate, and strain (ε_{yy}) contours for unidirectional (1D) MF40 2.5 % TRC composite.

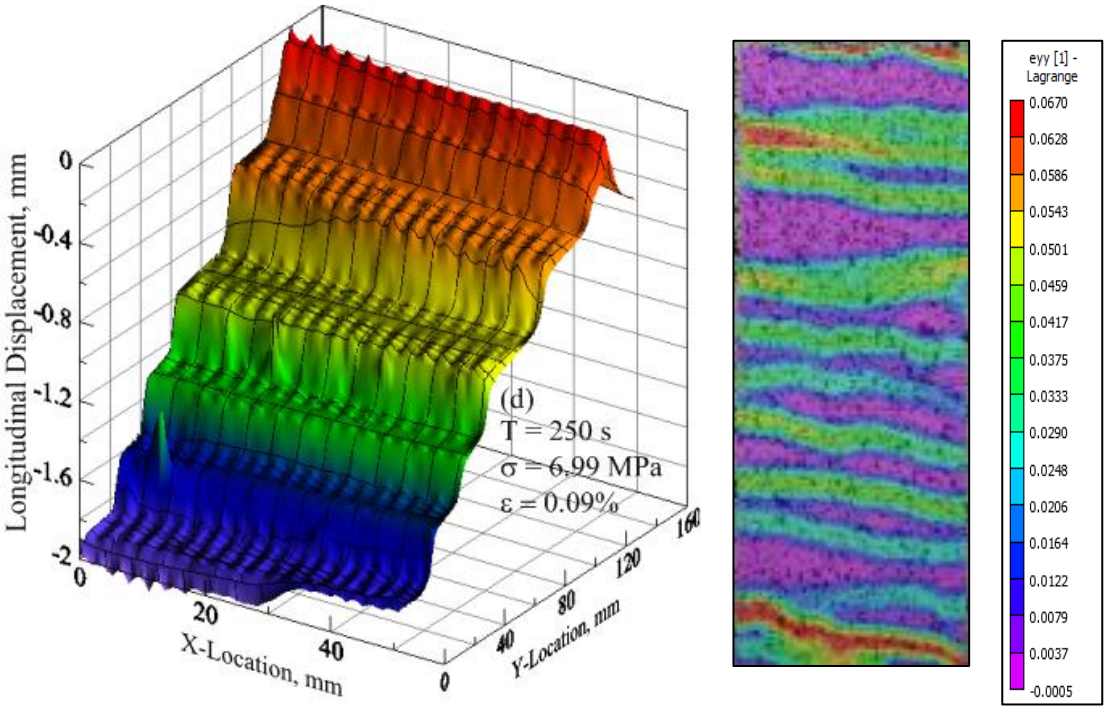

Figure 5(a). Displacement field for MAC 4% sample, discontinuity in longitudinal displacement demarcates the cracks developed along the width (X, mm) (b) Lagrange strain contours in Y direction for TRC laminate 4% open weave structure

2 STUDY OF POLYPROPYLENE FIBERS AND THEIR INTERACTION WITH CEMENT MATRIX

2.1 Introduction

Two types of proprietary polypropylene yarns manufactured by BASF Construction Chemicals, OH, USA were investigated in the current study as shown in Figure 1. Master Fiber MAC 2200CB is a commercial chemically enhanced monofilament macro-synthetic polypropylene (PP) fiber and is known for superior bond with cementitious matrices. (see Fig. 1(a)). MF 40 is a fibrillated PP with micro-synthetic yarns comprising of 500 thin filaments of 40 microns each (see Fig. 1(b)).

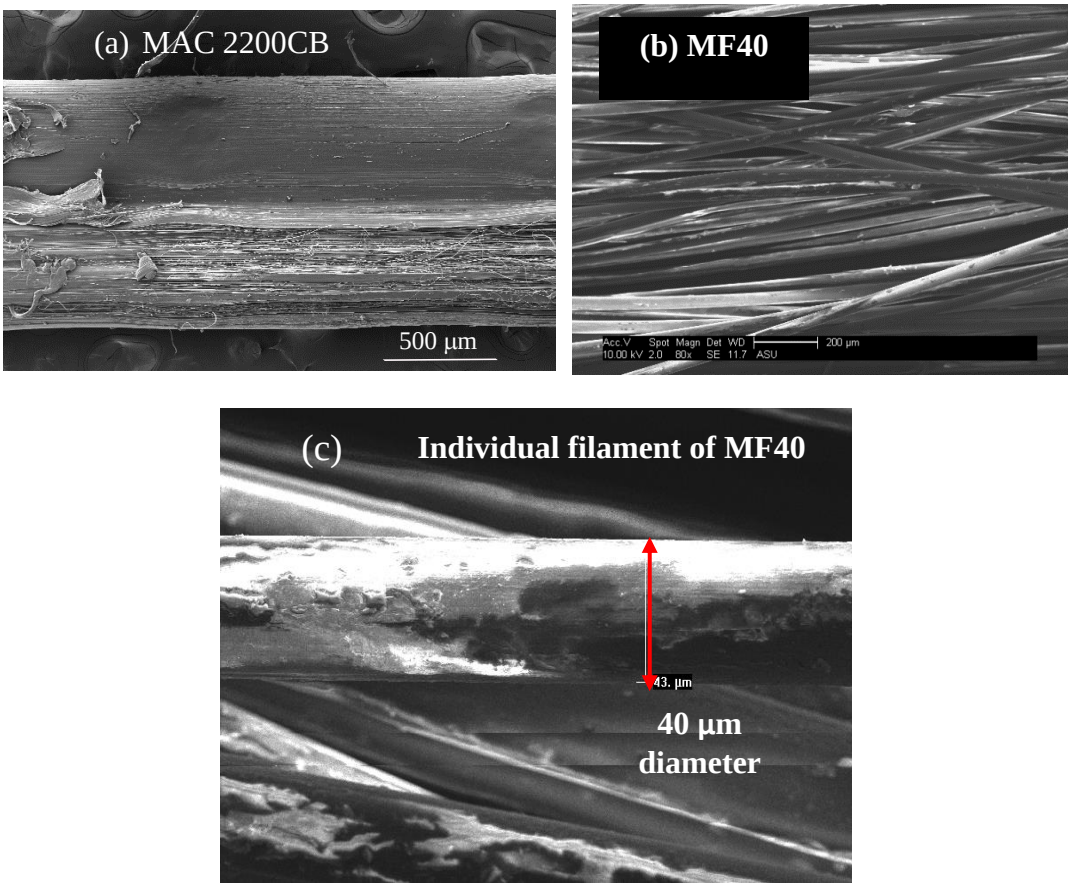

Figure 6 (a) Macro-synthetic MAC 2200CB fiber, (b) multifilament fibrillated microfiber(c) SEM image of fibrillated nature of microfiber MF40, 500 filaments comprise of a single fiber.

MAC 2200CB macro-fiber is used as a secondary reinforcement in cast-in place and precast concrete, slab-on-ground, pavements, and to control shrinkage and temperature cracking. The effective yarn diameter of MAC 2200CB and MF 40 were measured through image analysis of micrographs of fibers scanning electron and average diameter was reported to be 0.82 and 0.89 mm, respectively. A study was undertaken to understand the tensile response of the individual fibers, their interaction with cement matrix and their response as primary reinforcement in concrete laminates as unidirectional and textile reinforcements. This chapter elaborates on the tension response of fibers and their interaction with matrix. Quasi-static single fiber tests and pullout tests were performed and results were evaluated.

Fiber structure of MAC 2200CB is crimped monofilament as shown in figure below. The crimps are asymmetrically places on the front and back surface which forms an alternating wave over the side.

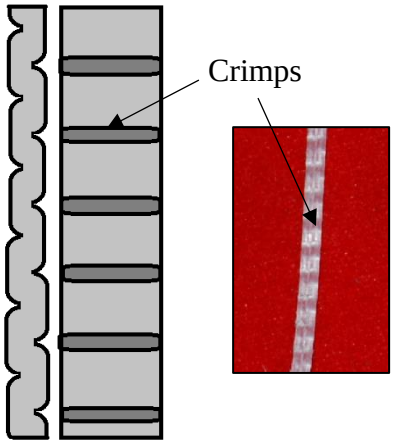

Figure 7. Macrostructure and fiber geometry of MAC fiber.

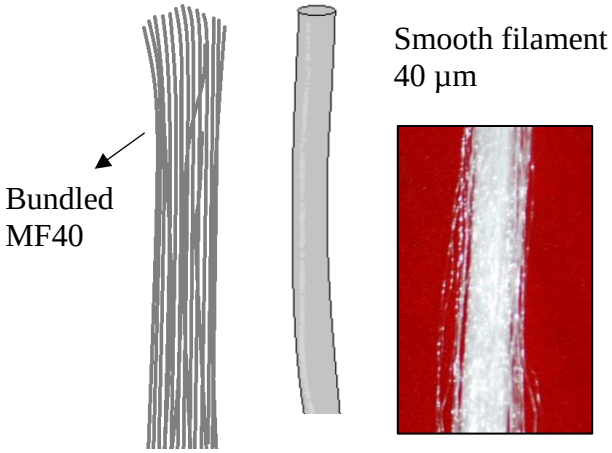

Figure 8. Fiber structure of multifilament MF40 with complete fiber and individual filament schematic.

Direct tension tests were performed on fibers using displacement controlled tests at a strain rate of 0.016 /min of on a minimum of 3 replicate fiber coupons at gage length of 152.4 mm, 203.2 mm and 254 mm. The setup is shown in Figure 2. A low capacity 1300

N (300 lb) interface load cell was used to measure the load while the strain measurement was recorded using the 50-mm gage length extensometer. The load cell proved to be more sensitive to fiber slip as compared to the actuator force response, indicating the quality of the test. Stress-strain properties measured from these tests are summarized in Table 1. A universal joint was connected to the testing frame to allow rotation of the grip and remove any potential bending moment. The universal joint also helps in the alignment of yarn during the test. To arrest the slip and capture true stress strain response of the specimen, grips as shown in the figure 3 were used. The fiber was fed and wrapped around the upper mandrel on the upper grip. After the cross head was moved to the gage length position, the fiber was aligned and wrapped along the bottom grip mandrel. The fiber was then secured in the mandrel using frictional wedge screws. The extensometer was mounted using rubber bands as shown in figure 3

Figure 9.Single Fiber Test Set Up

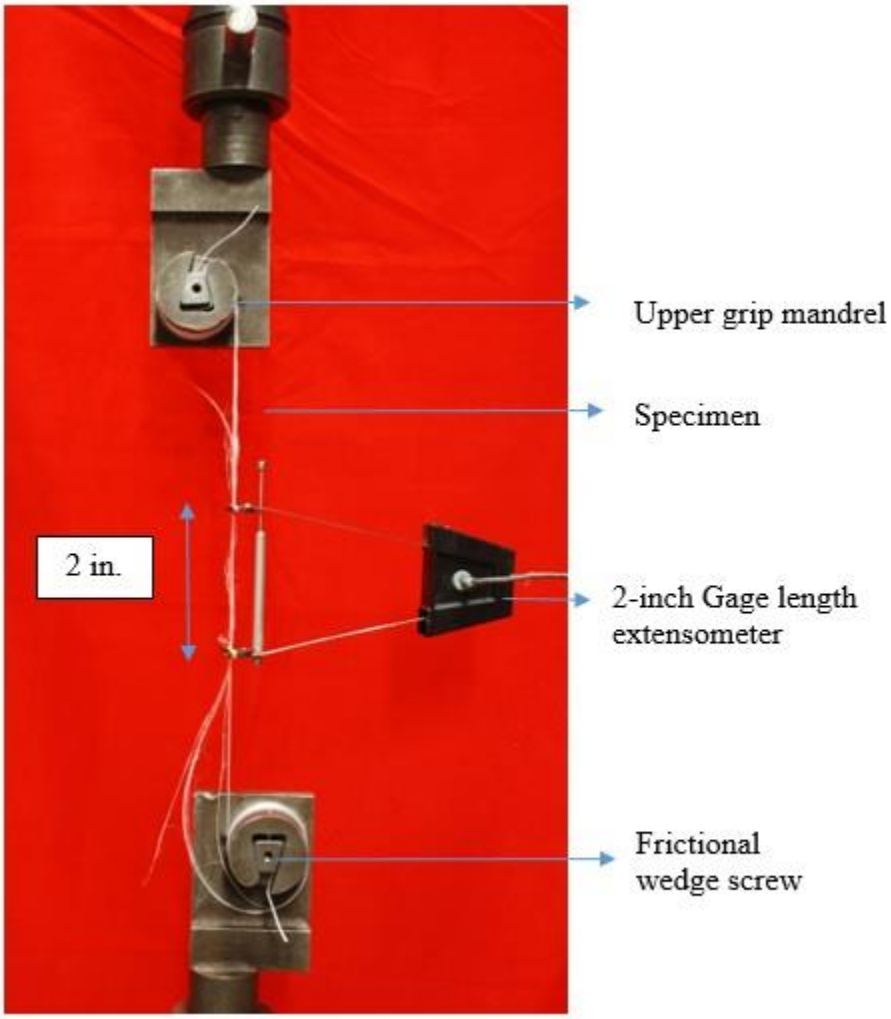

Figure 10.Specimen setup gripped and mounted extensometer showing failed MAC specimen

The study focuses on the understanding the shape, dimension and structure of the fibers and its effect on the tensile response which requires a contacting method of deformation measurement. The polypropylene fibers have a very smooth surface which are prone to slip at the mandrels as shown in figure 2. Mounting an extensometer directly on the fiber compensates for the error due to the slip and facilitates accurate characterization of fiber strain.

2.1.1 Test Set Up and Gripping Sets

The single fibers were tested on an MTS 810 frame under displacement control at a strain rate of 0.025/min. The specimen was not perfectly vertical before the test. This is due to the free tilt of the fixture in the presence of universal joint. However, as test starts and load increases the specimen aligns itself perfectly. Effect of gauge length, Young's modulus, peak stress and strain were measured.

2.1.2 Mounting the Specimen

The MAC fibers due to their stiff nature were easy to mount. The fiber of desired gauge length was first wrapped around the top grip which was secured by means of the wedge key. Once the fiber was tightly secured in the upper grip, the bottom actuator was aligned to achieve the desired gauge length and the fiber was wrapped around the bottom mandrel and secured. Special attention had to be paid to wrapping the MAC fibers so that there isn't any slip between the wrapped fiber. To achieve this, the furling was tight and aligned very close to each other such that no excess fiber was available for slip. The MF40 samples, due to their fibrillated filaments, provide a better frictional grip around the mandrels whereas, MAC fibers was prone to slippage. Once, the fiber was mounted in the grips, the 50.8 mm extensometer was mounted and secured with the help of rubber bands as shown in Figure 3.

2.1.3 Single Fiber Tension Experimental Plan

A set of 3 gauge lengths were tested for the two different fiber types. A constant strain rate of 0.025/ min was maintained for all the tests. The displacement rate was

calculated based on the constant strain rate for each gage length of samples to be tested. Table 1 summarizes the experimental plan undertaken for tensile tests.

Table 1. Experimental Plan for single fiber tensile tests.

Sr. No	Fiber Type	Fiber Gage Length, mm	Stroke Displacement Rate, mm/min
1	MAC, MF40	152.4	0.006
2	MAC, MF40	203.2	0.004
3	MAC, MF40	254	0.01

2.2 Results and Discussion

2.2.1 Comparison between MAC 2200CB and MF40

Test Results for MAC and MF40 fibers tested at 152.4mm shown in figure 4 The variation in the tests results ensures the repeatability of these tests and the standard deviation values give an estimate of the quality of the testing. The plots show tensile stress versus the stroke strain response. This response although does not yield the true response due to the slip in the grips. The extensometer strain over 50.8 mm of gage provides for a much accurate strain response. The stress versus extensometer strain is used to estimate the parameters.

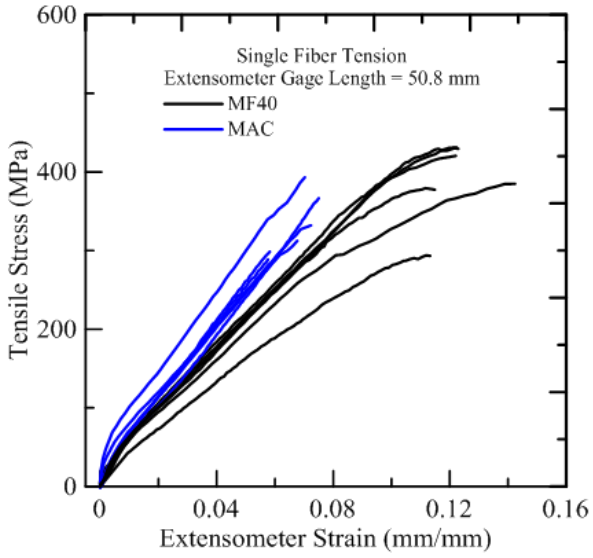

Figure 11. Tensile Stress Strain response of MAC versus MF40 fibers.

A bilinear stress strain response was observed for both the fibers exhibiting a stiffer response till a yield point beyond which stiffness reduces until failure. An initial elastic modulus, E1 and a post yield modulus, E2 are collected from the tests. The objective of the study was to understand the fiber behavior based on material moduli, strain capacity, ultimate strength, total toughness and failure pattern. Table 4 summarizes the experimental parameters for the single fiber tensile test for both the fiber types. The macro-synthetic fiber, MAC 2200CB has comparatively higher elastic modulus as well as post yield modulus or the plastic modulus measured up to failure. Due to a stiffer structure, MAC fibers exhibit a sudden failure compared to a progressive failure of each filament within the fiber bundle of MF40. Thus, the peak is evenly distributed at failure for MF40 and is defined by a sharp end for MAC. Figure 5 (a) shows the failed MAC 2200CB specimen compared to (b) MF40 microfiber.

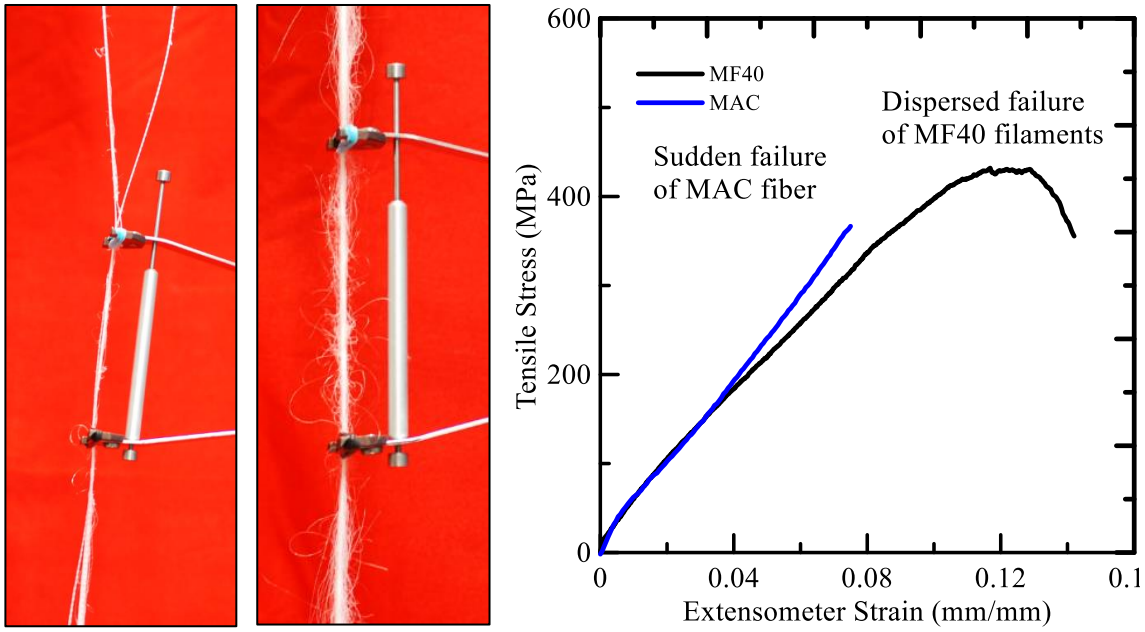

Figure 12. (a) Failed MAC fiber image, (b) Failed MF40 fiber (c) Tensile stress versus extensometer strain comparing MAC and MF40 failure.

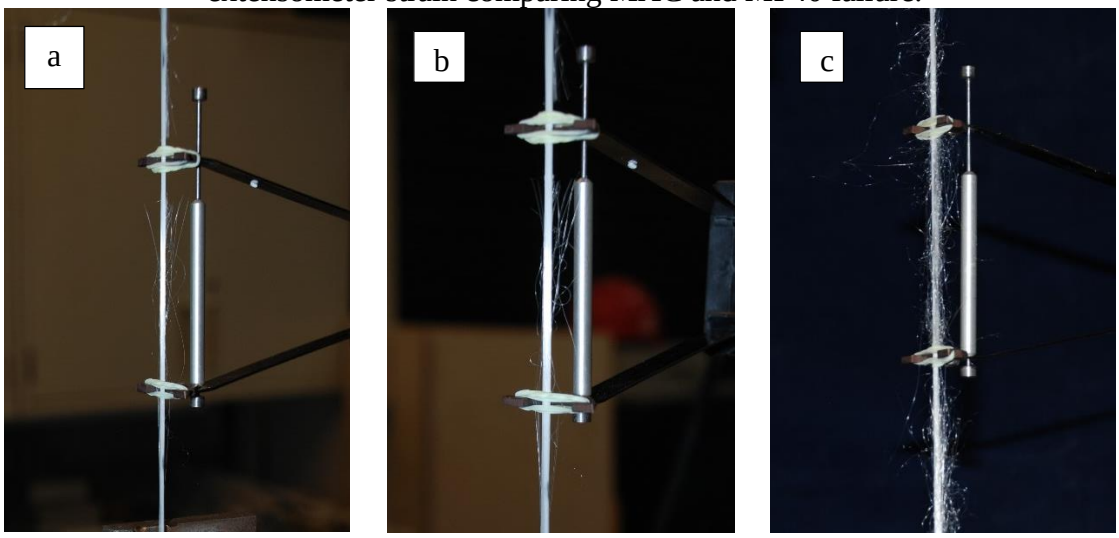

Figure 13. (a) Filaments breaking during the initial stage of the test, (b) Mid way through the test, (c) end of the test.

As mentioned earlier, the extensometer aids in arresting slip which is evident by the stress strain response shown in Figure 6(a). All the results parameters in Table ** have been calculated by using the extensometer displacement response.

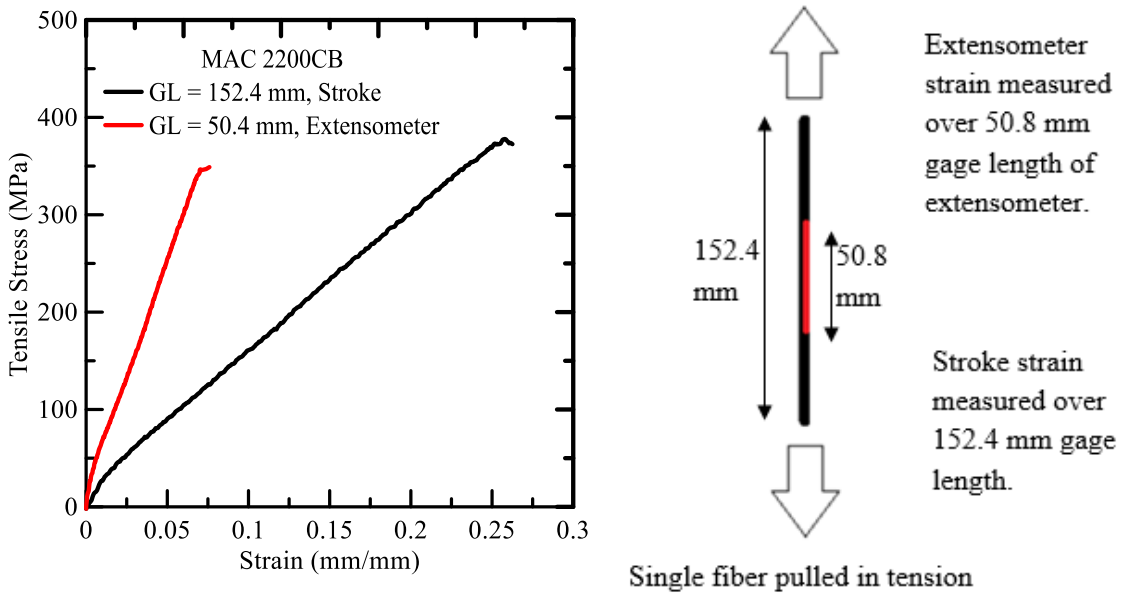

Figure 14 (a) Stress Strain curve showing extensometer strain versus stroke strain for a MAC sample.

The main difference between the two-fiber compositions is in the strain capacity of the microfibers with a toughness of MF 40 is twice of MAC 2200 CB. This is attributed to structural nature of MF 40 monofilaments which distribute the damage among the multiple fibers and fail progressively until the entire yarn fails. This leads to a higher strain capacity. The strain capacity is as much as 43% higher in MF than MAC. MAC 2200CB is inherently a stiffer fiber than the bundled MF40. The initial linear elastic modulus for MAC is 9.2 GPa whereas MF40 exhibits 5 GPa. The post yield reduced modulus for MAC is 4.6 GPa which is 50% higher than MF40 post yield modulus of 3 GPa. This higher stiffness for MAC 2200CB can be attributes to its inherent structural stiffness. The MAC fiber has a tubular structure with micro indentations on the surface and polymer resin surface coat. The finer MF40 fibrils are softer by their make and show no rigidity on its own. The work to fracture the bundled MF40 is significantly higher than that for MAC 2200CB primarily because each MF40 filament uniformly distributes the load within the filaments which

break sequentially over the failure strain range. Results show that MF40 is 2.2 times tougher in tension than MAC 2200CB due to its fibrillated nature.

Table 2. Single fiber test results for MAC and MF40 fibers, gauge length 152.4 mm

Sample	Max. Load	Max. Ext. Disp.	Tensile Strength	Elastic Modulus, E1	Post -yield Modulus, E2	Work to Fracture
MAC	N	mm	MPa	MPa	MPa	N.mm
T1	235.6	3.9	378.7	9602.8	4760.7	541.3
T2	250.3	5.8	402.3	8271.1	2940.3	1129.7
T3	245.1	3.6	394.0	7270.6	5149.8	454.6
T4	238.4	4.0	382.1	9547.5	4376.5	562.3
T5	280.8	3.7	452.4	12472.8	5641.9	709.7
T6	221.4	5.4	354.9	8272.1	4524.7	800.7
Avg	245.3	4.4	394.1	9239.5	4565.7	699.7
Std.Dev.	20.0	0.9	32.8	1812.8	918.3	244.6
MF40	N	mm	MPa	MPa	MPa	N.mm
T1	238.8	5.7	329.3	3648.8	2375.9	1354.3
T2	278.8	5.6	384.4	4365.1	2856.3	1926.6
T3	313.9	6.3	432.8	5043.8	3445.6	1673.5
T4	318.3	6.7	438.9	6637.1	3488.0	1504.2
T5	285.6	7.4	393.7	5897.2	2700.8	1665.4
T6	327.2	6.1	451.1	4318.4	3482.4	1399.7
Avg	293.8	6.3	405.0	4985.1	3058.2	1587.3
Std.Dev.	33.0	0.7	45.5	1111.7	479.3	212.2

2.2.2 Effect of Fiber Gage Length on Tensile Response

Tensile test results for the three fiber gage lengths are shown in figure 8 and9. Extensometer strain is plotted with stress for 3 gage lengths. Due to the slippery nature of MAC monofilament the results vary for different gage lengths and do not follow a general

trend. To estimate the true response of such fibers, a smaller representative gage length should be used.

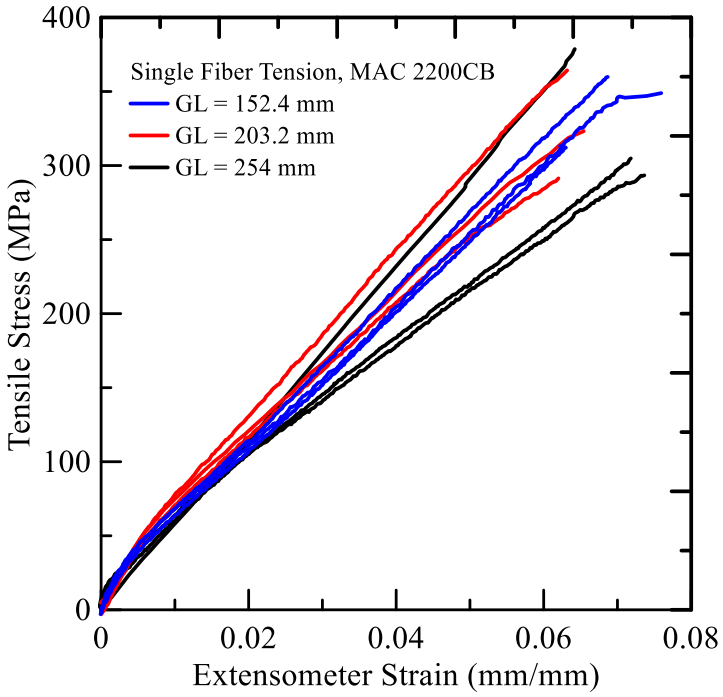

Figure 15.. Effect of fiber gage length on stress strain response for MAC fibers

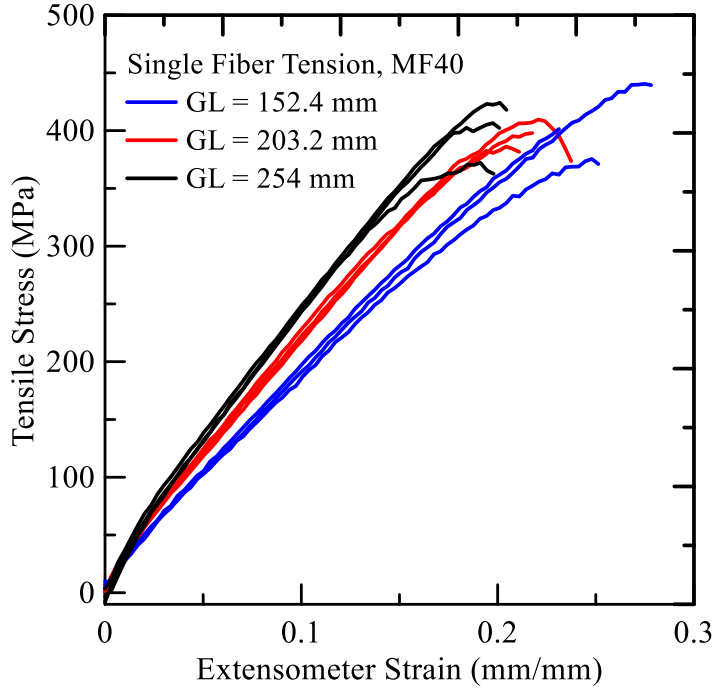

Figure 16. Effect of fiber gage length on stress strain response for MF40 fibers

MF40, on the other hand does not slip due to its fibrillated filament nature. Typically, a stiffer response is expected with increasing gage length of fiber. MF40 shows this behavior with increasing gage length. 254 mm long fibers show a constant peak stress with lower peak strain for higher gage length. This can be attributed to the size effect of the fibers as more fibers start fraying over a longer gage resulting in excessive straining early on.

We can conclude that MAC fiber is a higher modulus fiber, which is tough due to its geometry and stiff due to its monofilament nature. However, as a bundled fiber, MF40 despite being a lower modulus fiber displays excellent strain range during failure which provides for a higher toughness. Thus, characterizing the fiber properties is necessary to understand the further aspects of their behavior with cement as a composite.

2.3 Fiber Pullout and Interface Characterization

Enhanced composite behavior is primarily governed by interfacial bond characteristics between fiber and matrix. Matrix interface plays a very important role in controlling mechanical properties of cementitious composites. Bond characteristics of fiber-cement systems using analytical and experimental techniques have shown to be the most significant parameter that characterizes the interface parameters and toughening mechanisms [23,24]. Peled et al reported that the bond is highly dependent on geometry of the fabric and its geometry. [25]. The modulus of elasticity of the yarns as well as the geometry of the reinforcing yarns contributes to the pullout behavior and bonding of the various systems. [26]. This calls for a detailed study of fiber matrix interaction for monofilament MAC and MF40 microfiber bundle, before one can compare their composite

behaviors. Interfacial bond characteristics between fibers and matrix, and can be quantified by performing fiber pullout tests.

An experimental and analytical investigation was performed to measure the pull-out resistance of fibers from blended cement matrices. The effect of curing age, fiber embedded length, fiber and matrix types on the fiber-matrix interface and rate sensitivity were studied. This study is confined to comparison of polypropylene single yarns - MAC 2200CB, monofilament crimped polypropylene fiber and MF40, a straight microfiber bundle consisting of fibrillated filaments. A series of samples were prepared based on combinations of fiber type, fabric embedded length EL, mixture type and crosshead displacement rate of pullout. Pullout tests were conducted to determine interfacial shear bond of fiber reinforced concrete.

2.3.1 Mix Designs

Two different types of matrix mixes were used in the study. A control matrix consisted of cement paste of ordinary Portland cement. To enhance the workability of the mix 0.1% superplasticizer was added. Another matrix consisting of 15% Type F fly ash by weight of cement was used to study the effect of fly ash on bonding. Table 1 presents the mix design for the pullout samples.

Table 3. Mix formulation for matrix

Mix ID	Mix Design	Cured	Fiber Types	Fiber Embedded Length (mm)
A	1C:0.4W	7	MAC, MF40	7.6,12.7,19.05
B	1C:0.15 FA 0.4W	7	MAC, MF40	7.6,12.7,19.05

2.3.2 Sample preparation

All specimens were cast in a PVC mold of 12.7 mm diameter, 50.8 mm height with varying embedded lengths of fibers. The specimens were cast using wooden supporting molds which held the fiber at the required embedded length and the concrete was poured after placing the sample on the wooden mold. Figure shows a schematic diagram of the pullout sample with the matrix core and an embedded fiber

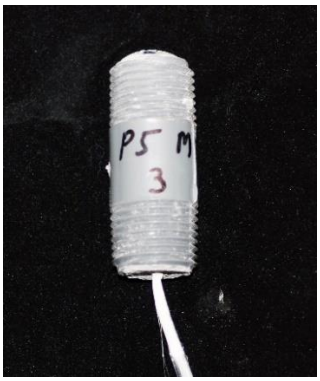

Finished pullout specimen with MF40 fiber

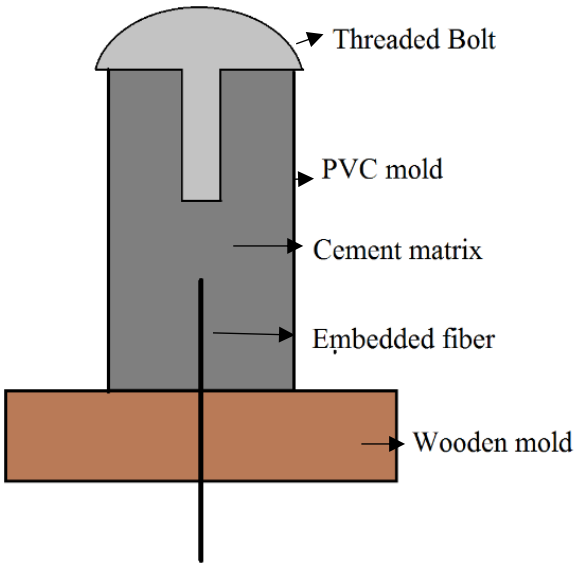

Figure 17. (a) Finished MF40 specimen, (b) Schematic of the specimen during casting

2.3.3 Step by step procedure for sample preparation

1. First clean the wooden mold and orifices before rowing the fiber through the mold.
2. Bring the fiber to the desired embedded length and secure the loose end by tape.
3. Once all the fibers are ready, place the PVC molds around the fibers.

4. Pour the matrix in the PVC mold using a syringe. Cover the cast sample with a threaded bolt with a rounded head to anchor the matrix on the top edge.
5. Remove the tape from the other end and remove the sample from the wooden mold after 24 hours of casting and cure as per the age requirement.

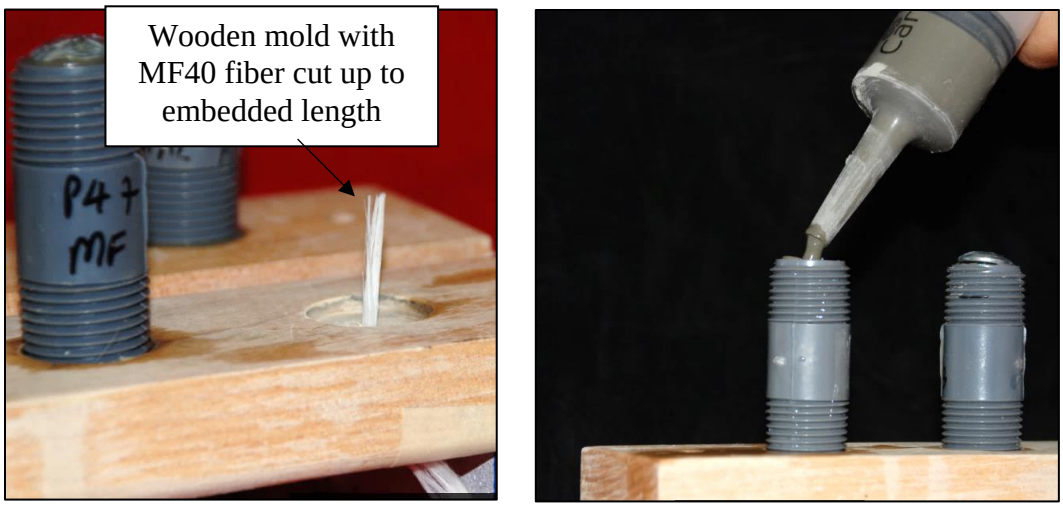

Figure 18(a). Wooden mold with MF40 fiber of desired embedded length. (b) cement matrix being poured in the PVC mold containing fiber by means of a syringe.

Special care had to be taken while pouring the cement paste as the fibers were to be kept straight while pouring cement. The fiber was held inside a small hollow plastic tube so that the cement being poured from top does not disturb the fiber orientation. Compacting the cement paste while pouring is necessary to avoid air entrainment in the mix which may affect the integrity of core and the interface resulting in incoherent bond strength estimation. It can also cause the core to be pulled out by the fiber while testing. All samples are tested for 7 days of curing.

2.3.4 Test apparatus

The test set up consisted of a fabric grip as shown in the figure which secured the loose fiber end by means of three screws. A thin copper sheet was used to safeguard the fiber from failing in the grip due to the tightening of the screws and distributing the grip evenly on the fiber face. The bottom of the fiber grip was connected to the stroke actuator using a connecting pin as shown. A 300-lb. load cell was used to record the pullout force. A calibration factor pf 128.86 lbs./V was used to convert the raw data into the load cell response in force units. A 0.15-inch range of gage length extensometer was used to record the slip between the matrix and the fiber end. The extensometer was mounted using stiff rubber bands to reduce slip. The top arm was in contact with the core and the bottom arm was placed on the fiber grip thus ensuring slip of fiber from the core. The fiber was mounted close to the fiber end achieving negligible free length between the sample and fiber grip such that a true load slip curve can be obtained which will not require any correction for the free length elongation

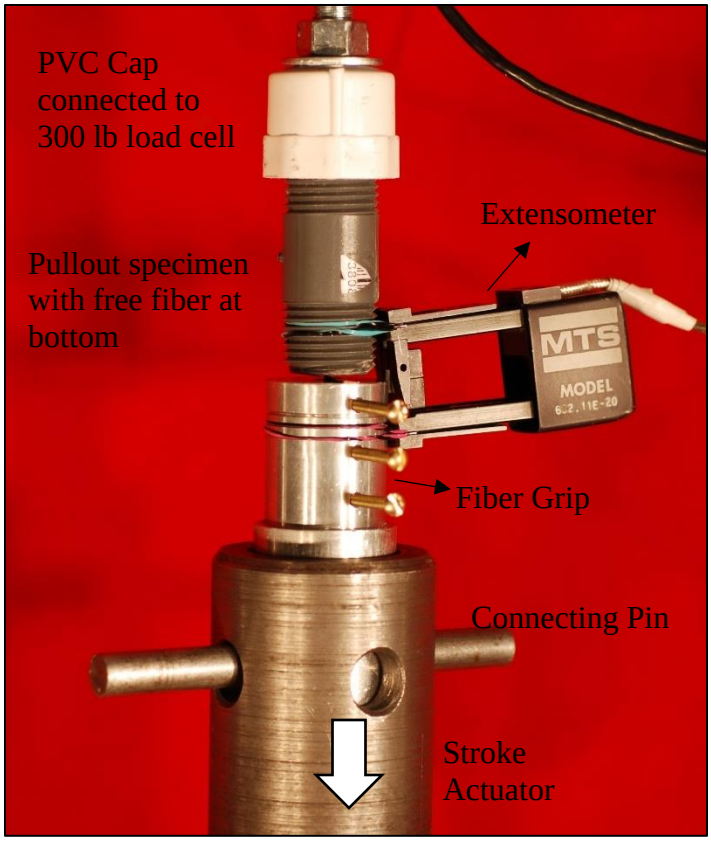

Figure 19. Test Setup for fiber pullout tests.

2.3.5 Pullout Test Procedure

Pullout tests were carried out on a MTS 810 at 3 different static crosshead rates of 0.021, 0.21 and 2.12 mm/sec. The experiment was designed to get at least 3 replicate plots for every sample group. However, due to inconsistency in fiber behavior, matrix formulations etc. several matrix cores were pulled out of the PVC molds while testing. Samples disturbed while setting up or misaligned tests were discarded. Following images show the test progress for a MAC fiber.

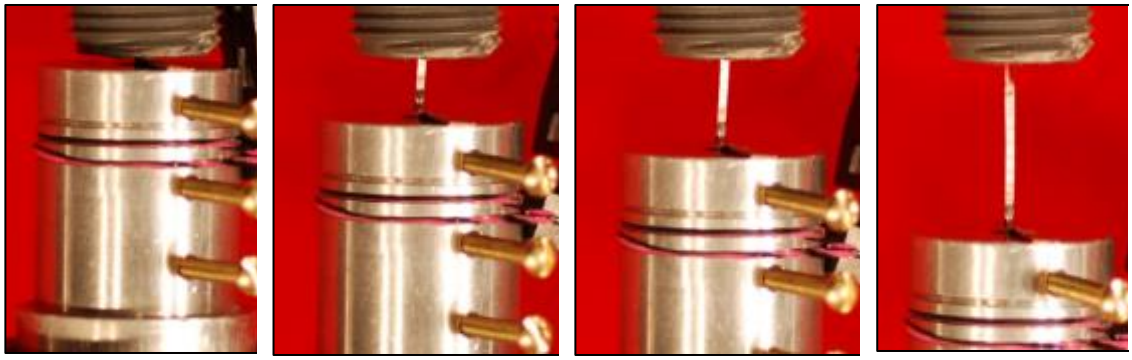

Figure 20. MAC fiber being pulled out as the test progresses.

Due to the small range of the extensometer, the test had to be paused and extensometer removed before the test could proceed. This caused a kink in the load slip response due to fiber relaxation, which had to be accounted for while processing the data. The PVC core was first mounted in the threaded PVC cap and tightened to avoid any slip. The free fiber was then pulled through the fiber grip and secured by means of the three screws as mentioned above. The set up was then aligned and connected to the bottom actuator. The extensometer was then attached as shown on a PVC sleeve around the core to measure the local slip of the fiber. The following load slip curve shows the extensometer vs. stroke slip. The extensometer response was used to measure the initial stiffness of the sample and the remaining parameters were estimated from the stroke response. Figure * represents the load slip response for a control mix (Mix A) MAC sample with an embedded length of 7.6 mm.

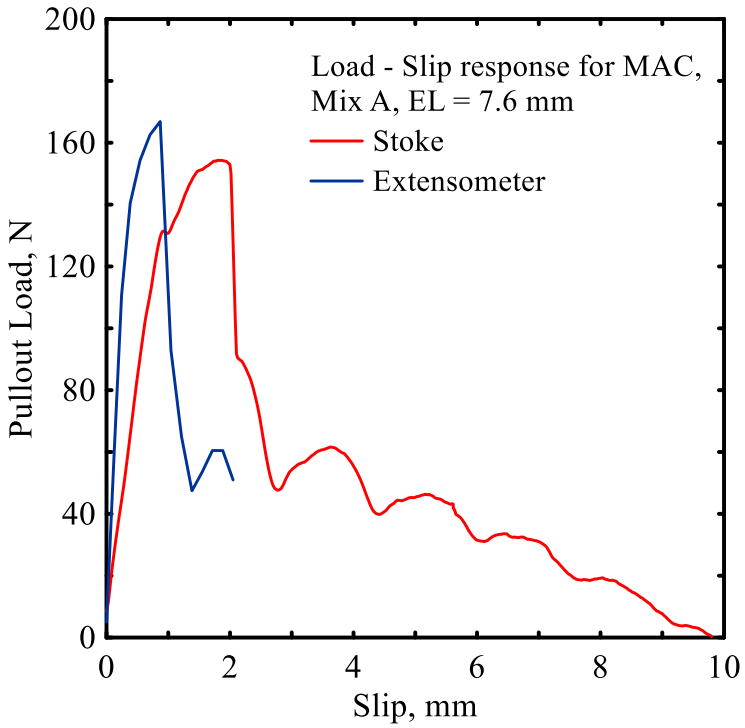

Figure 21. Load slip response comparing stroke displacement with extensometer displacement. The extensometer response is used to estimate the material parameters.

2.3.6 Results and Discussion

2.3.6.1 Fiber structure

The efficiency of different types of fiber structures can be judged by the pullout resistance provided by the nominal cross sectional area available for resistance [27]. A series of tests were performed and experimental data was analyzed to understand the difference in the fiber response. Figure 15 represent the primary difference between pullout response for the crimped PP MAC fiber and the multifilament MF40.Due to the indentations on the fiber, the MAC fiber displays undulations after debonding. These bumps are periodic in the frictional slip region and its effect is directly observed as an enhanced toughness in that region. Peled et al. [28] reported that the crimped geometry of polypropylene fibers may generate improved bonding and that the maximum pullout

resistance was a function of the wave length and amplitude of the waves in the crimped structure of the fiber.

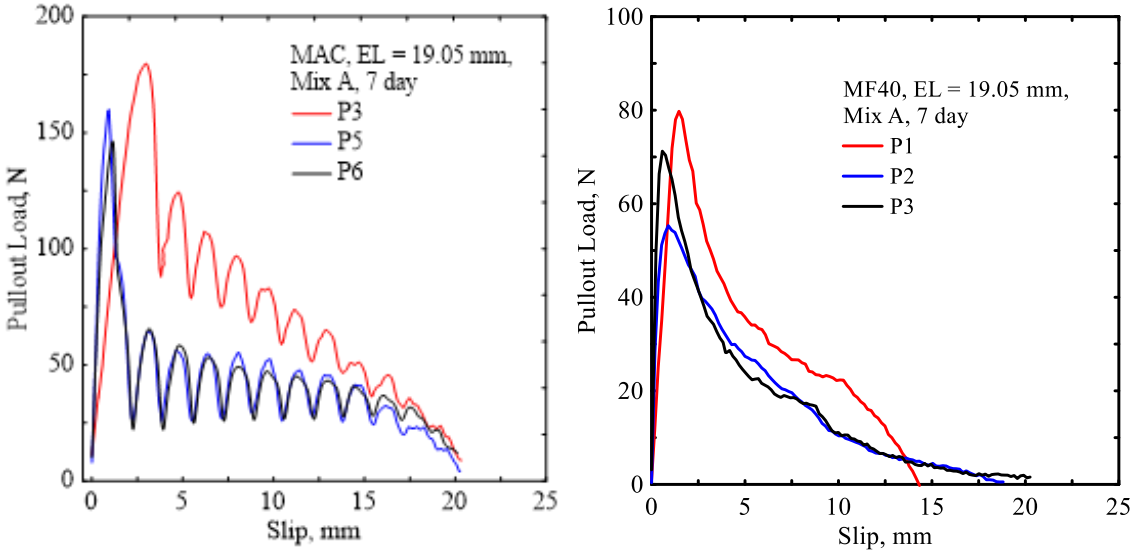

Figure 22. Comparison of pullout load slip response for MAC and MF40 tested for Mix A at displacement rate of 0.02 mm/sec for 7 day samples.

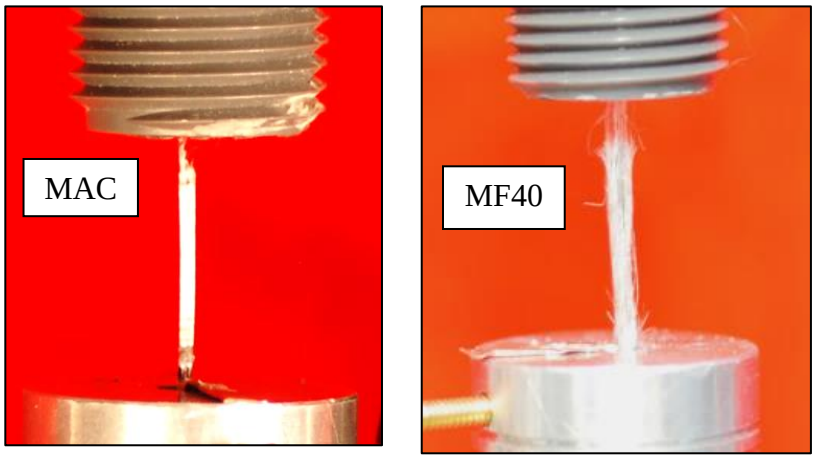

Figure 23.(a) MAC monofiber pulled out of the matrix core, (b) Filaments of bundled MF40 pulled out at the end of the test.

However, the bundled microfiber has a higher stiffness despite being a lower modulus fiber and the post debonding region of the curve drops smoothly as the bundle completely slips. In almost all microfiber tests, it was observed that some of the peripheral

filaments were bonded to the matrix even at the end of the test. This indicates that due to its bundled nature, MF40 enhances bond as a unit, but once filaments start failing or slipping, the toughness drastically reduces whereas MAC slips uniformly over every indentation.

It can also be suspected that due to the different surface treatment of these fibers their bonding with the cement matrix can be different despite the material being the same. The stress transfer of a bundled fiber is complex and cannot be accounted in terms of an average bond. Bartos [29] proposed a telescopic effect in which external elements which are well bonded to the matrix may fracture and the internal ones engage in slip. This can be observed in the MF40 samples. Thus, to enhance MF40 behavior it is necessary to pultrude the filament bundle through a cement matrix such that efficient bonding can be achieved. Use of fillers was suggested to increase the sleeve to core ratio for MF40 like bundled fibers to improve their bond with cement matrix by Cohen et. al. [30]. Figure 24 shows the telescopic effect manifesting within a bundled fiber.

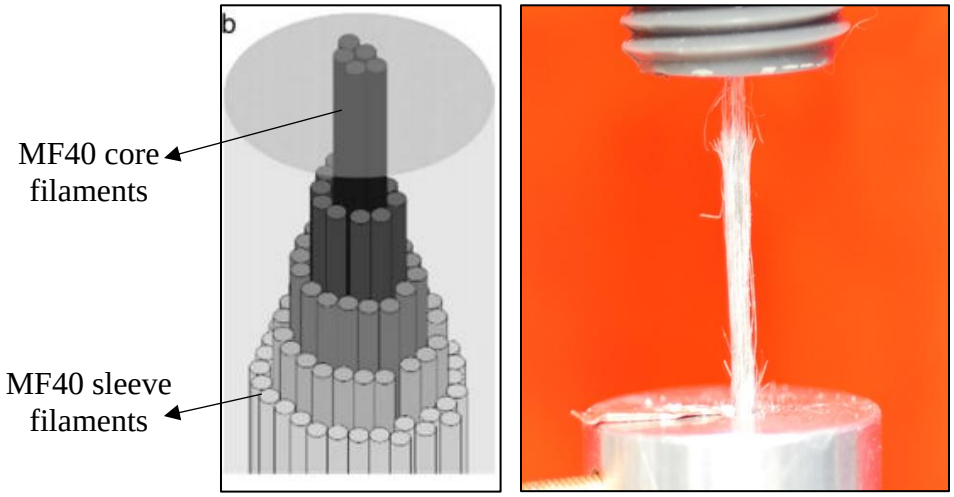

Figure 24. Telescopic effect observed in MF40 fibers where sleeve filaments fracture whereas core filaments get pulled out.

2.3.6.2 Effect of Embedded Length

Three embedded lengths of 7.6, 12.7 and 19.05 mm were considered in the study for both MAC and MF fibers. The load slip response for the control mix is shown in figure 17. The embedded length contributes to an increased interfacial shear strength due to a higher area of contact with the matrix. Thus, the force required to initiate debonding is increased with a deeper fiber embedment. Due to the homogenous nature and make of MAC, the forces are in near proximity for varying embedded lengths. Peak load for MF40 increases by 60% due to the embedded length. This can be attributed to higher specific surface area of the filaments in contact with the matrix A higher embedded length of MF40 increases the interfacial contact and thus the shear strength as a function of the filaments.

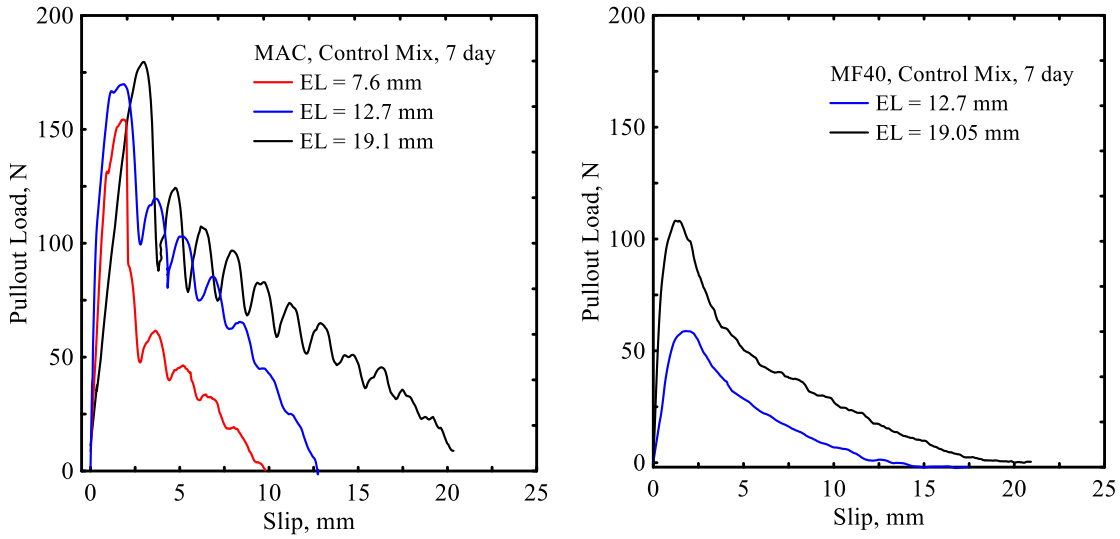

Figure 25 Load Slip response for 3 embedded lengths for (a) MAC and (b) MF40 for the control matrix tested at 0.02 mm/sec.

2.3.6.3 Effect of Matrix Mix

Plain cement paste matrix (Mix A) was compared with fly ash blended matrix (Mix B). MAC fibers at 19.05 mm embedded length showed distinct improvement in the bond with fly ash mix. MAC fibers did not debond and started failing in the grip. The response of the fiber being pulled in tension and slipping after failure can be compared with the uniaxial single fiber tensile response

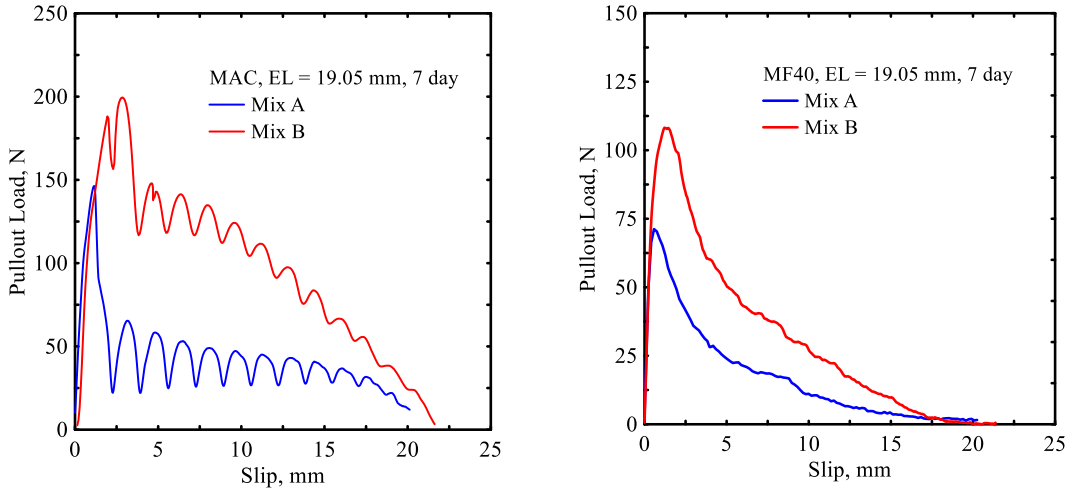

Figure 26. Effect of fly ash mix on MAC and MF40 fiber pullout response.

2.3.6.4 Strain sensitivity of fibers during pullout:

Several studies have emphasized on the behavior of polypropylene at varying strain rates due to its inherent polymeric nature and viscoelastic properties. It is necessary to study the strain sensitivity of the fibers keeping in mind the rate at which they may be pulled in a composite. 3 different strain rates of 0.02,0.2 and 2.1 mm/sec were considered in the study with the first two rates being in the quassi static range and 2.1mm/sec accounting for an impact pullout force. The slow rate tests help in characterizing the energy flow and toughness parameters, whereas the high strain rate gives an estimate

about the elastic property of the fiber matrix as a unit. The first two rates hence show similar pullout strength and toughness for the MAC fibers. At 2.1 mm/sec the fiber is pulled out and the strength is overestimated. Figure 19 and 20 shows the response of MAC fibers 12.7 mm embedded length tested at the three strain rates. A higher slip of the fiber is noted in this rate. The microfiber study for the strain rates is to be added to this section.

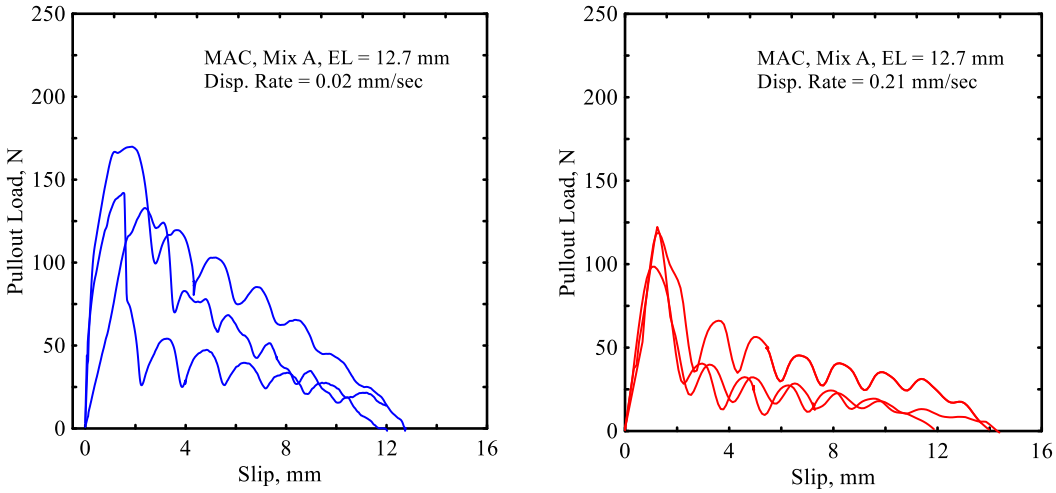

Figure 27. Pullout load slip response for slow slip rate of 0.02 mm/sec and 0.2 mm/sec for MAC fibers embedded at 12.7 mm in Mix A.

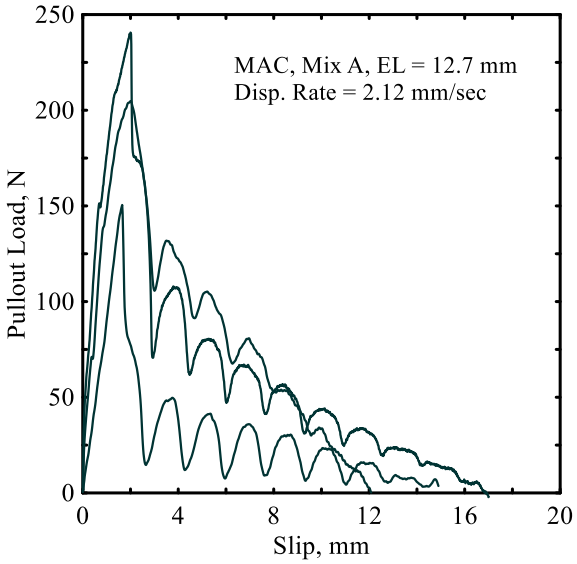

Figure 28. Pullout load slip response for fast slip rate of 2.1 mm/sec for MAC fibers embedded at 12.7 mm in Mix A.

2.4 Conclusion

The study indicates that bonding efficiencies in polypropylene fibers depend on variety of factors other than fiber geometry. Both the fibers behave differently with the matrix based on their structure and matrix mix. Fly ash effects may be more evident at a later age in the pullout samples as early age fly ash mix does not densify the interfacial transition zone between fiber and matrix completely at 7 days. Additional testing is required at 28 days of curing to confirm the bond enhancement due to fly ash.

3.MECHANICAL RESPONSE OF UNIDIRECTIONAL POLYPROPYLENE CEMENT COMPOSITES

3.1 Introduction

In this study filament winding technique was employed for manufacturing unidirectional thin laminates with continuous polypropylene fibers. The automated manufacturing system comprises of state-of-the-art integrated stepper motors, motion control and data acquisition. The system utilizes the full potential of fibers and reduces cost of labor intensive tasks of manual construction products. Effect of two different fiber types, structure and matrix formulation is studied. Mechanical response of unidirectional (UD) composites are measured in terms of tensile strength, crack spacing, and degradation of stiffness as a function of applied strain. Matrix formulations consisted of blended cementitious matrices containing various proportions of Type II OPC, sand and fly ash as a control matrix mix. Effect of additives such as chopped glass microfibers and sub-micron wollastonite fibers were evaluated as hybrid matrix. Three different volume fractions of continuous yarns were studied. Mechanical tests were performed on continuous fiber composites under uniaxial tension and four-point bending.

3.2 Manufacturing Process – Filament Winding Methodology

A filament winding system developed at ASU for manufacturing continuous fiber cementitious composites. This versatile system can be easily configured to produce unidirectional, cross-ply, and angle ply laminates and pultruded sections. Computer-aided manufacturing provides the flexibility and control for developing structural applications. The mechanical components of the system consist of the feed, guide, and the take up (mold) sections as shown in figure 21.

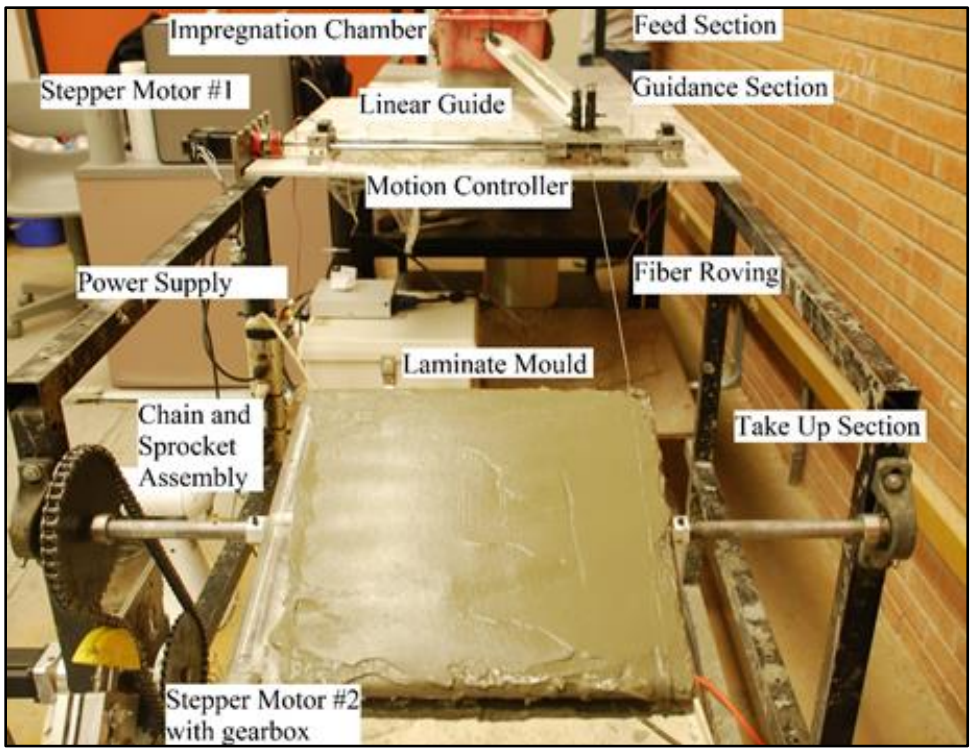

Figure 30. Filament Winding Setup at ASU.

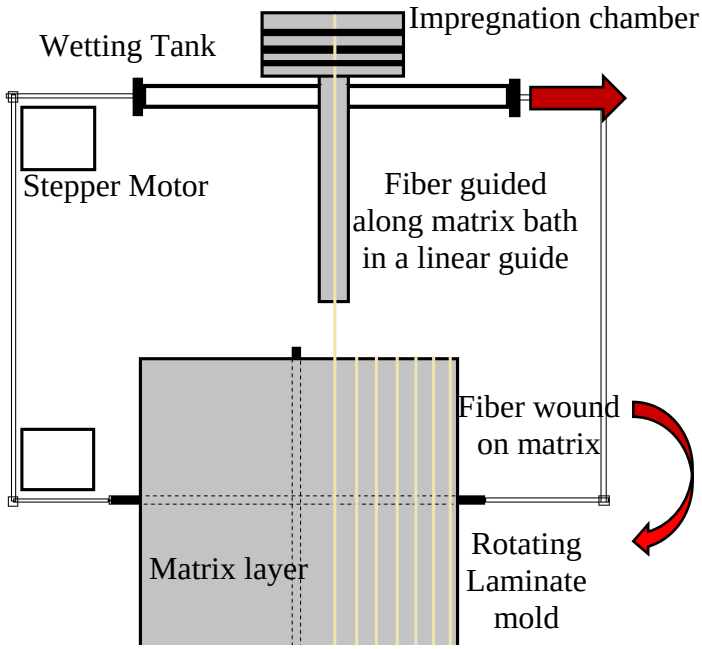

Figure 29. Schematic depicting filament winding along the mold

3.3 Mix Design

To evaluate the unidirectional composite laminates a control mix consisting macro-fiber MAC 2200 CB and multi filament MF 40 fibers with three different volume fractions of 1%,2.5% and 4% were studied. The experimental plan is summarized in Table 2. Direct tension tests and four-point bending tests (marked with *) were conducted on minimum four replicate samples for each mix design. Specimen groups marked with a plus sign (+) were tested after 7 days of curing. Hybrid blended mixes, HM:1-3 with wollastonite fibers (NYAD-G) substitution of 10% of cement, and alkali-resistant glass (ARG) micro-fibers at 1.5% by volume were also developed.

Table 4. Groups of specimens with continuous fibers developed in the study

Group ID	**Yarn Type**	**Yarn V_f%**	**Matrix Composition**
I, II*, III	MAC	1.0, 2.5, 4.0	Control Mortar
IV+, V*+, VI	MF 40	1.0, 2.5, 4.0	Control Mortar
VII	MAC	2.5	Hybrid Mortar 1 (HM 1): AR Glass
VIII*	MAC	2.5	HM 2: Wollastonite
IX*, X*	MAC, MF 40	2.5	HM3: Wollastonite + AR Glass

The control mortar mix design used a blend of 48% Portland cement type I/II, and 15% by weight of class F fly ash, Sand/Cementitious material ratio of 0.45, and a water/binder ratio of 0.35 as shown in table 5.

Table 5. Mix design used for control mix with MAC 2200 CB and MF40 continuous fibers.

Material	Weight Fraction (%)
Portland Cement (Type I/II), C	48%
Fly Ash (Class F), FA	7.2%
Fine Silica Sand, S	24%
Water, W	20%
HRWR (BASF Melflux)	0.03%

Hybrid blended mixes, HM:1-3 with wollastonite fibers (NYAD-G) substitution of 10% of cement, and alkali-resistant glass (ARG) micro-fibers at 1.5% by volume were also developed. Mix design of hybrid mix, HM-3 is shown in Table 6.

Table 6. Mix design used for hybrid mix of glass micro-fibers (ARG) and wollastonite sub-micro fibers (Wol).

Material	Weight Fraction (%)
Portland Cement (Type III/IV), C	45%
Fly Ash (Class F), FA	7%
Fine Silica Sand, S	23%
Water, W	18%
Wollastonite (NYAD-G), Wol.	4.5%
Glass Microfibers (Nippon), ARG	2.2%
HRWR (BASF Melflux)	0.03%

3.4 Specimen Preparation

The filament wound mold was mixed using the mix design specified in section 1.2. Once the mold was cured, samples were harvested out of the mold by cutting it as per the

required dimensions. Samples were then speckled to perform digital image correlation which will be explained in the next chapter. The LVDT was mounted on the sample by means of two aluminum collars attached on the sides. Quick hardening glue was used to attach the collar and the LVDT was mounted.

3.5 Tensile Tests on UD Composites

The setup used to conduct coupons tension tests with nominal dimension of 300x62x13 mm is shown in Figure 1(a). Direct tension tests were performed using a closed loop servo-hydraulic testing frame operated under stroke control, while the applied stress and specimen elongation was recorded throughout the test.

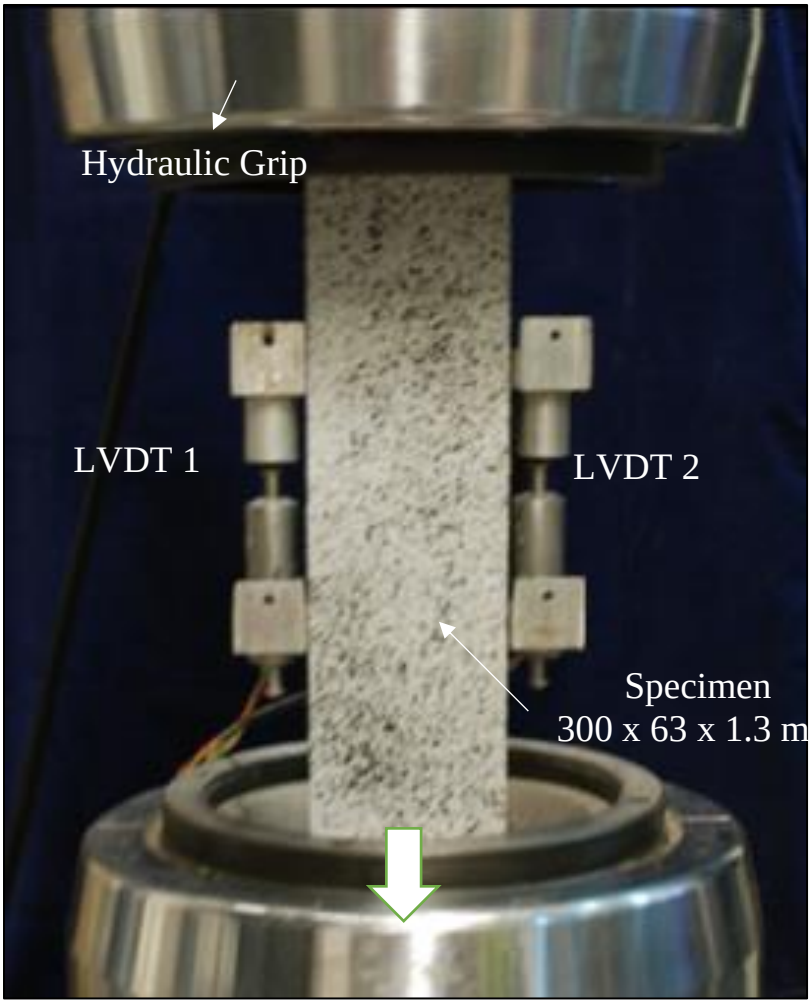

Figure 31. Tensile test setup for filament wound UD composites

Specimen was held using hydraulic grips with the pressure maintained between 1.7 to 2 MPa. Elongation of the specimen along 90 mm of gage length was recorded using two LVDTs of 6 mm range (± 0.5 mm). These LVDTs were mounted on both sides of the specimen and the average response was used for strain evaluation. The experimental data was analyzed using a MATLAB program for data reduction, smoothening and calculation of important test parameters. Elastic modulus E and post crack modulus E' is calculated using the LVDT response to gage the sample strain, whereas the toughness at different

strain levels is calculated using the stroke response of the actuator as it measures the entire response of the sample. Figure shows the LVDT and stroke response comparison which reflects how the LVDT response disengages due to its shorter range.

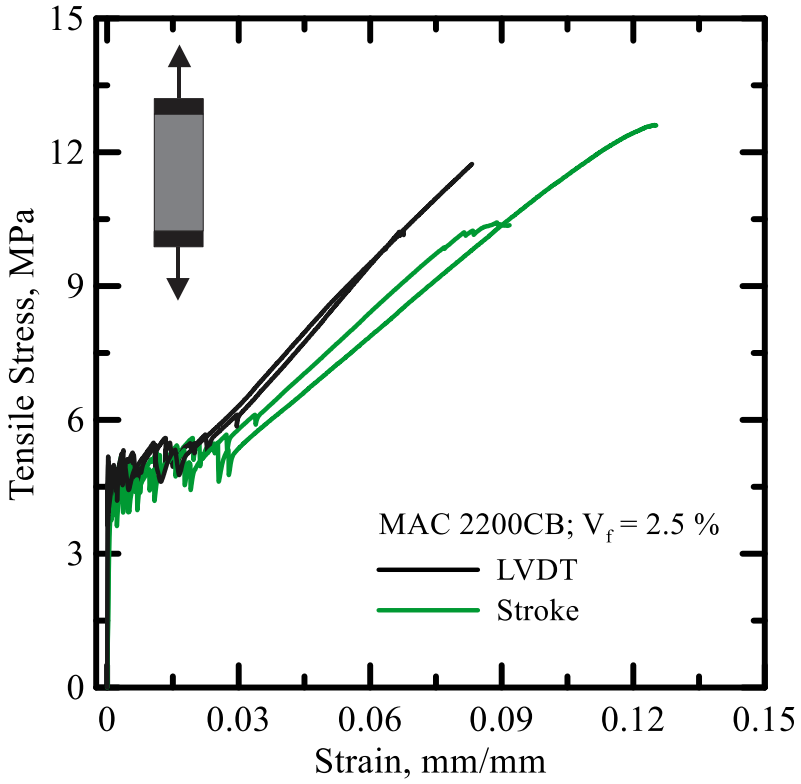

Figure 32.Comparison of LVDT and actuator response of MAC 2200CB at 2.5% in tension

Tensile Response of UD composites:

The typical stress-strain response is presented in Figure 33 and classified into three stages. Stage I represents the linear elastic region and ends at the formation of first crack The matrix and fiber behave linearly, till the matrix starts cracking and stress is transferred to the fiber. In this zone, there exists an iso- strain relation between the fiber and matrix and the strain distribution along the longitudinal and transverse directions is uniform.

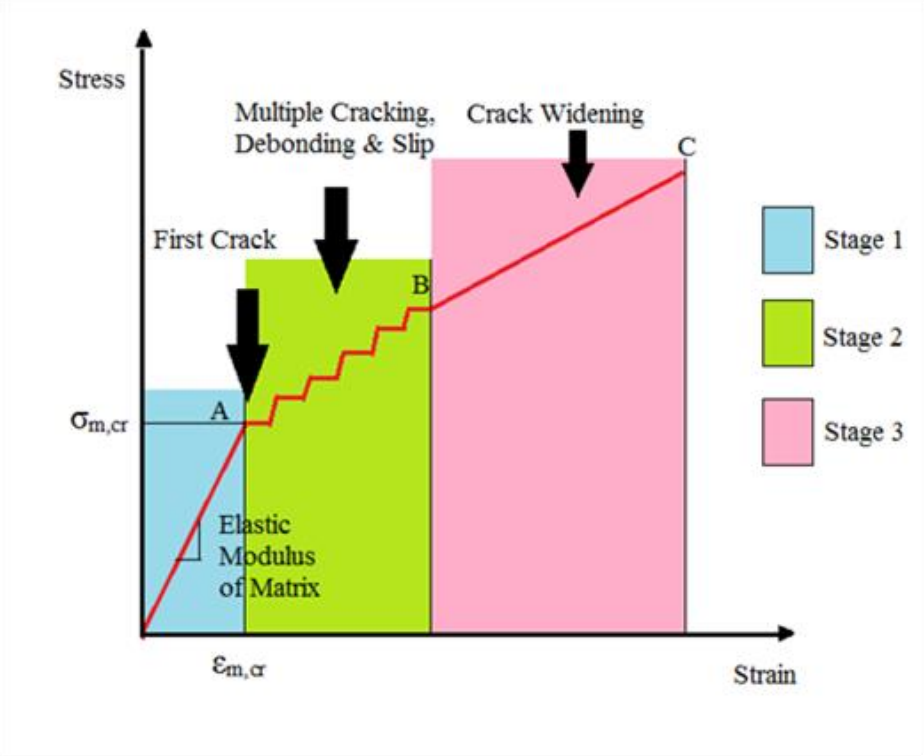

Figure 33.Tensile Stress Strain response classified into 3 stages.

Several studies on tensile response of FRC show 4 distinct zones with transition between BOP – and BOP + stress levels as zone 2. Due to the low fiber content, the experimental data for these tests do not show a clear transition between BOP- to BOP + till the first crack propagates through the specimen width. Hence, this zone is idealized as stage I which terminates at the first crack. This zone characterizes the elastic modulus, the first crack strength and strain for the composite. Beyond the first crack, formation of multiple parallel cracks dominate zone II. Stage II starts after the first main through-crack, and initiates the dominant strain hardening behavior as shown by a series of parallel cracks that appear along the gage length of the specimen. The overall stiffness of the composite can be assessed by this range. The fibers present in the system bridge the cracks and allow for formation of new sequential cracks. The spacing and width of these cracks in this stage depend mainly on the fiber type, bond parameters and volume fraction of fibers. This stage

ends with fiber debonding and slip. Once formation of new cracks stops, the cracks begin to widen, matrix stress reduces, fibers begin to debond and are either pulled out or fracture. The tensile response for both MAC and MF40 composites with a control matrix at various fiber dosages exhibit these three distinct stages. Reproducibility of experimental data is shown in Figure 34 (a) and (b), where in tensile response of replicate test coupons of MAC 2200CB fibers and MF40 fibers are shown respectively.

3.6 Results and Discussion

3.6.1 Effect of Fiber Volume Fraction

The stress- strain response of the composites at different volume fractions are summarized in table 7. Effect of volume fraction of fibers on tensile properties is more pronounced for MF40 composites as all mechanical properties increase significantly as the dosages increases from 1-4%. Because the latter zone in Stage I depends on the dosage of fibers available for bridging, the first cracking stress is higher for laminates with a higher volume fraction of fiber for both MAC and MF40. MAC shows an average 1.4 MPa stress level for 1 and 2.5% fiber dosages. However, at 4% MAC dosage, the stress at first cracks increases significantly to 2.6 MPa. The MF40 fibers on the other hand have a lower first cracking stress of * MPa for 1% fiber dosage and an average of 4MPa for the 2.5% and 4% replicates.

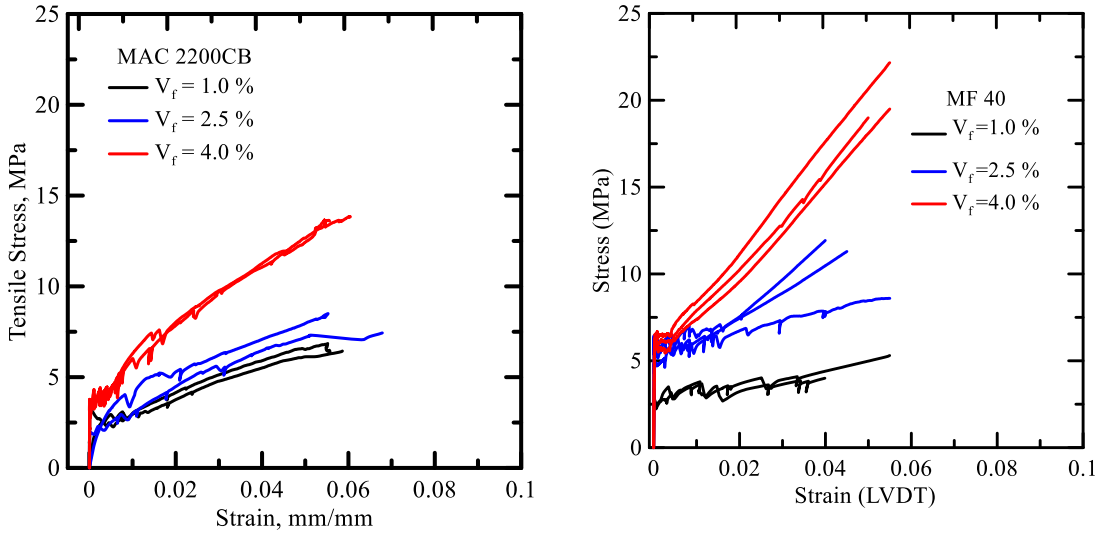

Figure 34. Replicates of continuous fiber cement composites with MAC and MF40

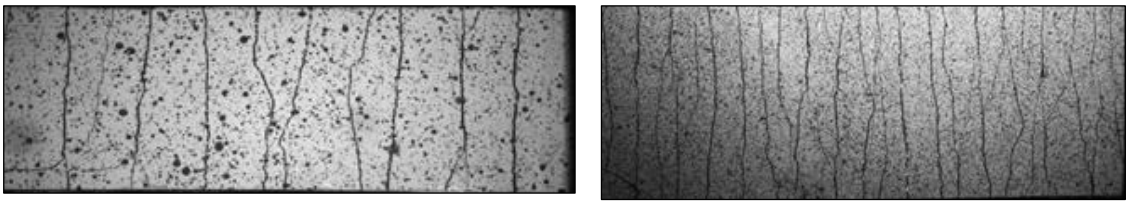

MAC 4% (#7)

MF40 4% (#3)

Figure 35. Images of samples showing multiple cracking

The ultimate tensile strength increases for MAC 2200CB replicates varies from 7.45 – 13.2 MPa, post cracking stiffness increases from 81-197 MPa, and overall toughness increases from 0.79 – 0.83 MPa. MAC fibers at 1 and 2.5% fiber dosage show similar stress strain behavior whereas at 4%, the overall composite stiffness and mechanical properties show improvement. The MF40 composites show stiffer post crack response with distinct distributed cracking for 1 and 2.5% fiber dosages. However, for 4% MF40 dosage, several fine cracks close to each other result in a high crack density and toughness. The first cracking stress for 2.5 % and 4% fiber dosage MF40 specimen is within 3.8 to 4.4 MPa, ultimate stress is 12.5 to 17.5 MPa and toughness is 1.1 MPa to 1.37 MPa which is 65% higher than MAC fibers at 4% dosage.

Table 7. Stress Strain response parameters for control mix laminates with different fiber dosages.

		MPa	mm/mm	mm/mm	mm/mm	GPa	MPa	N.m	MPa
Fiber Type, Vf	Sample ID	Stress at First Crack	Strain at First Crack	Strain at UTS	Ultimate Strain	Young's Modulus (LVDT)	Post-Crack Modulus	Work to Fracture (Stroke)	Total Toughness (Stroke)
MAC 1%	#1	1.3	0.0006	0.12	0.16	2.0	94	90	0.79
	#2	1.3	0.0007	0.13	0.16	1.8	70	89	0.79
	#6	1.4	0.0003	0.13	0.15	4.7	80	65	0.75
	Avg	1.3	0.0006	0.13	0.16	2.8	81	89	0.79
MAC 2.5%	#2c	1.1	0.0008	0.13	0.17	1.3	88	143	0.98
	#4	1.5	0.0001	0.07	0.12	11.7	110	57	0.39
	#5	2.0	0.0002	0.12	0.16	9.8	180	131	0.94
	Avg	1.5	0.0004	0.11	0.15	7.6	126	110	0.77
MAC 4%	#5	2.0	0.0002	0.08	0.09	12.9	170	146	0.74
	#6	3.1	0.0002	0.08	0.11	20.9	170	205	0.93
	#7	2.6	0.0002	0.10	0.10	16.9	250	160	0.82
	Avg	2.6	0.0002	0.08	0.10	16.9	197	170	0.83
MF40 1%	#2	1.6	0.0003	0.13	0.14	5.4	36	96	0.53
	#3	2.3	0.0016	0.13	0.14	1.4	38	102	0.56
	Avg	1.9	0.0009	0.13	0.14	3.4	37	99	0.55
MF40 2.5%	#3	3.2	0.0002	0.13	0.17	20.4	120	170	0.90
	#5	4.1	0.0001	0.12	0.13	30.8	140	211	1.26
	#8	4.6	0.0002	0.08	0.12	24.6	206	168	0.77
	Avg	4.4	0.0002	0.10	0.13	27.7	156	190	1.01
MF40 4%	#3	4.2	0.0001	0.11	0.12	31.8	190	259	1.42
	#5	4.1	0.0002	0.10	0.12	21.6	200	220	1.23
	#7	3.1	0.0002	0.13	0.14	17.1	200	271	1.46
	Avg	3.8	0.0002	0.11	0.13	23.5	197	250	1.37

3.6.2 Effect of Fiber Type

The results from the instrumented tensile tests on the two-polypropylene based continuous fiber structures: MF 40 and MAC 2200 CB is shown in Figure 3. MF 40 as discussed earlier has fibrillated fiber structure resulting in enhanced bonding with the cementitious matrix. The abundant open spaces in the multiple filaments of MF 40 fibers allow for easier penetration of the cementitious matrix inside the fiber structure, resulting in superior mechanical performance.

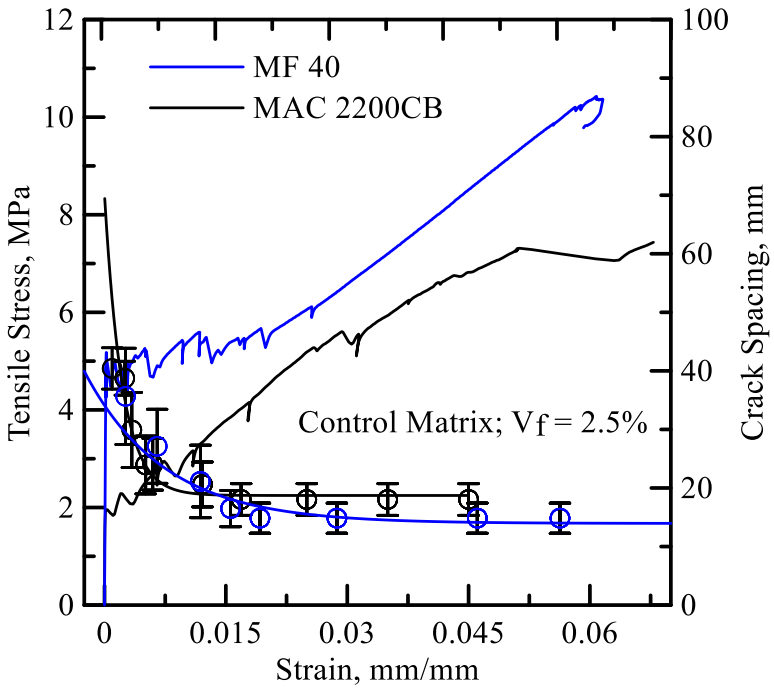

Figure 36. Tensile response of composites with MF40 fiber versus those with MAC fiber

This results in tensile strength over 10 MPa for laminated composites with continuous MF 40 fibers. MAC being a mono-filament macro-fiber however provides limited improvement in the performance of the composite, despite its engineered structure. Tensile strength of about 8 MPa is evident in composites with MAC fibers. Crack spacing - strain response also reported here implies that the denser cracks with smaller individual

crack spacing and lower saturated cracking is evident in composites with MF 40 fibers, compared to MAC fibers. This again suggests the MF40 fibers bond more effectively with the cementitious matrix resulting in finer distributed cracks along the gage length.

3.6.3 Effect of Hybrid Cement Mix

The addition of short fibers and wollastonite resulted in an appreciable increase of the first cracking strength, ultimate tensile strength, and strain capacity of the composite shown in figure 37 The addition of glass fibers results in a brittle composite are generates a response like the control matrix. However, addition of wollastanite helps in development of stable parallel cracking and an enhanced post crack response.

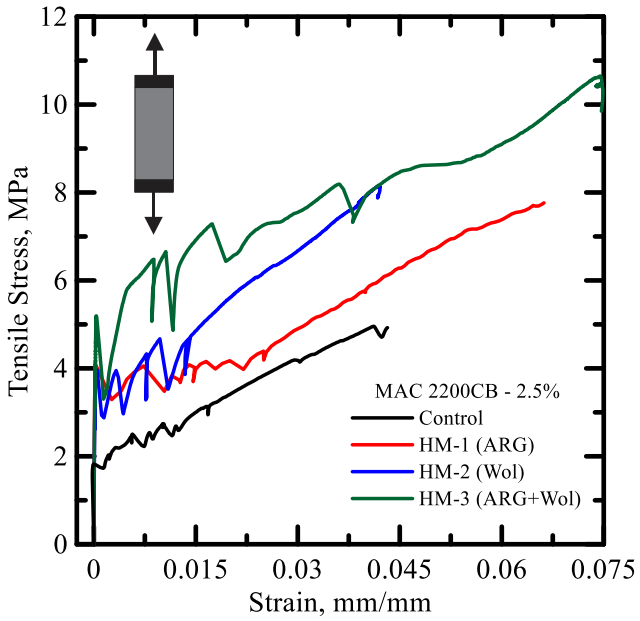

Figure 37 Effect of hybridization of matrix for MAC 2.5% UD composites.

Hybrid mix 3 on the other hand has a higher first crack stress, wider distributed cracking zone and achieves toughness up to 10 MPa. This can be attributed to the strengthening effect of matrix by the submicron wollastanite particles which help in better

bonding and delay debonding and pullout for the fibers. Thus, addition of AR glass and wollastanite helps in increasing the overall composite response significantly. Figure 38 shows the stage 4 images for samples with hybrid mixes. Multiple cracking can be effectively prolonged by matrix modifications.

The following images depict the damage induced in the specimens at failure.

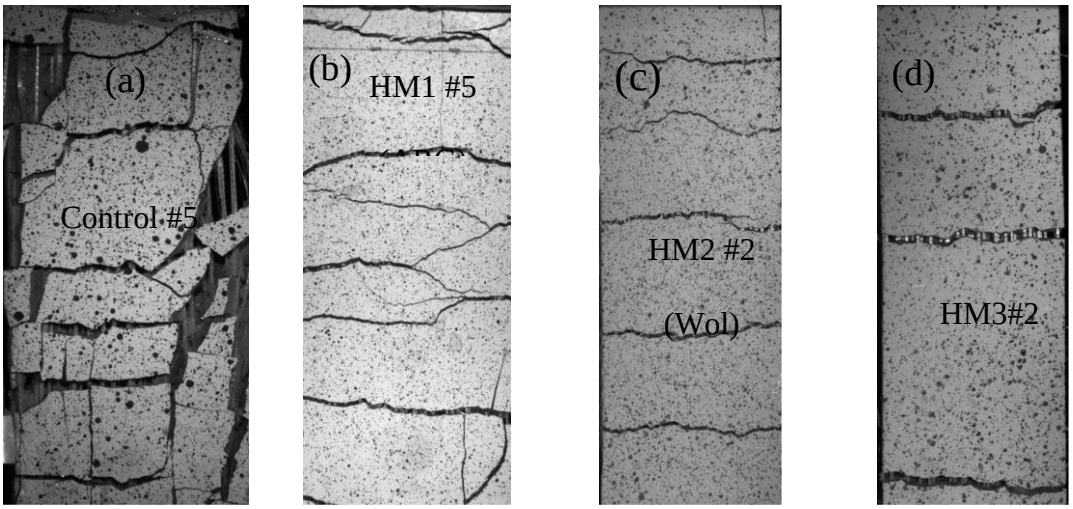

Figure 38.Extent of cracking in tension specimens with MAC 2200CB (a) control matrix, (b-d) hybrid matrices

3.7 Toughening Mechanisms in Fiber-Cement Composites

The fiber reinforcement within the composites aid to improve the toughness and ductility of the specimens through several strengthening mechanisms namely distributed parallel cracking, crack bridging, fiber pullout and fiber failure. As specimens are pulled in tension, the fiber-matrix interface prevents fracture through a series of distributed cracks transverse to the direction of the load thereby giving the composite higher ductility and toughness capacity.

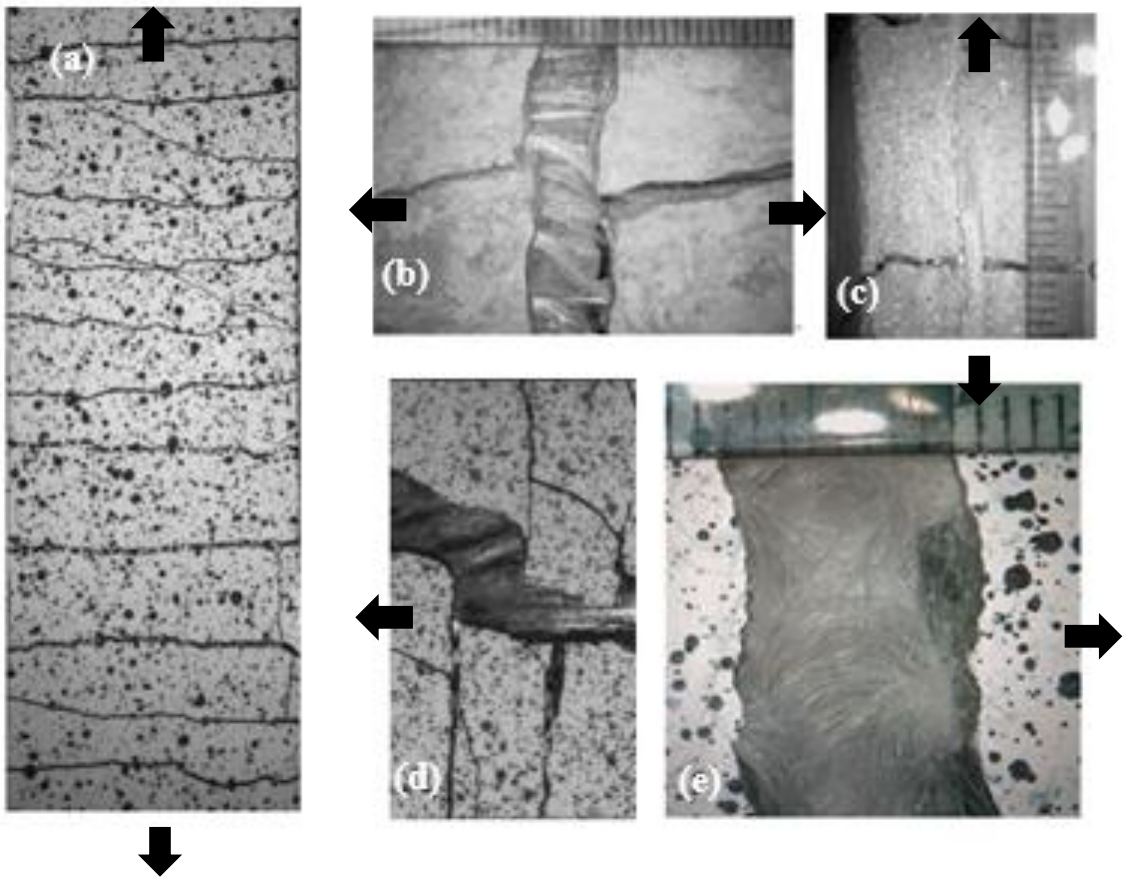

Figure 39 (a)Distributed cracking in MAC 4 % composite laminates under tension at crack saturation, (b) MAC fibers bridging the crack across sample width, (c) along thickness. (d) MF40 fibers being debonded and pulled out (e) MF40 filaments buckling after unloading. (All scale markers correspond to 1 mm)

The distributed crack patterns for fiber reinforced specimens pulled in tension can be seen in Figure 39 (a) for MAC 4 % sample. Crack bridging is the other key toughening mechanism within continuous fiber composites which can be shown along the width and thickness of a MAC2200CB sample in Figures 39 (b) and (c), respectively. The fibers prevent significant strains and relaxation of the composite by bridging the distributed cracks and thereby slowing crack propagation which allows for higher toughness. Figure 39(d) shows MF40 fibers being delaminated and pulled out along with transverse cracking along the fiber direction. The bond exhibited by MF40 is superior which results in fiber fracture accompanied by pullout. Figure 39 (e) shows the crack bridging provided by MF

40 fibrillated fibers which being to buckle after unloading as the matrix compresses the fibers. Fiber pullout is irreversible and the final stage of tensile failure.

3.8 Conclusion

The comparison of MAC and MF40 unidirectional laminates shows the multiple cracking behavior as the dominant toughening mechanism. MF40 due to its high strain capacity and higher energy absorption helps in enhancement of the composite response. MAC on the other hand shows a stiffer initial response. The elastic and post peak modulus for both these systems is in range of 2 to 23 GPa which is exemplary for a low fiber modulus brittle matrix composite. The hybridization of the matrix mix can help in strengthening the matrix properties and prolog the matrix softening stage. Additional matrix modification studies are required to fully comment on its effect as the study calls for additional replicate plots.

Toughening mechanisms in the multiple cracking, debonding and pullout zone of composite response is evident from the sample images. Use of transverse reinforcement can arrest the cracks developed along the width of the specimen. Next chapter deals with MF40 textile reinforced composites and their study in tension.

4.MECHANICAL RESPONSE OF TEXTILE REINFORCED CEMENT LAMINATES

4.1 Introduction

Unidirectional textile reinforced laminates exhibit excellent in plane but poor inter-laminar properties. This is due to lack of reinforcement in the thickness direction and leads to poor damage tolerance in the presence of inter-laminar stress.

Textiles are generally woven, knitted or braided from single or multifilament yarns before they are infiltrated by the concrete matrix. The extent of penetration of the cement into the bundle spaces depends on the structure and the density of the weave. The lengthwise yarns (warp) and crosswise yarns (weft) are at right angles with each other. Various factors make woven textiles more attractive than unidirectional fibers or other types of textiles. For example, the tightening of the joints that connect the weft and fill yarns induced by the junction points of the fabric strongly hold the filaments of the bundle and prevents them from being opened. Paste penetration into multifilament yarns leads to better fiber matrix bonding which improves strength. This form of textile reinforced system (TRC) could be easily adopted and modified to fabricate different structural shapes such as channels, angles, hollow sections and rectangular plates of any desired length and cross-sections. Open weave is a basic one-face warp in which a knit is worked from one fully threaded warp. In the first row the thread forms a stitch on the first needle; in the second row this occurs on the third needle. Stitches are made alternately, first on one side, then on the other. In tricot weaves one thread forms stitches alternately in two neighboring columns. By the pulling of loops, stitches are made alternately on one side, then on the other.

This study focusses on the open weave and tricot weave comparison of TRC manufactured using MF40 fibers. The effect of textile dosage in tension is also studied. Multiple cracking behavior of textiles in tension is compared with MF40 unidirectional laminates They provide an orthotropic to the laminate which cannot be achieved by use of unidirectional fibers as it exhibits poor strengths transverse direction. Textiles thus provide a dimensionality to the laminate with the ease for flexibility and enhance the overall composite behavior.

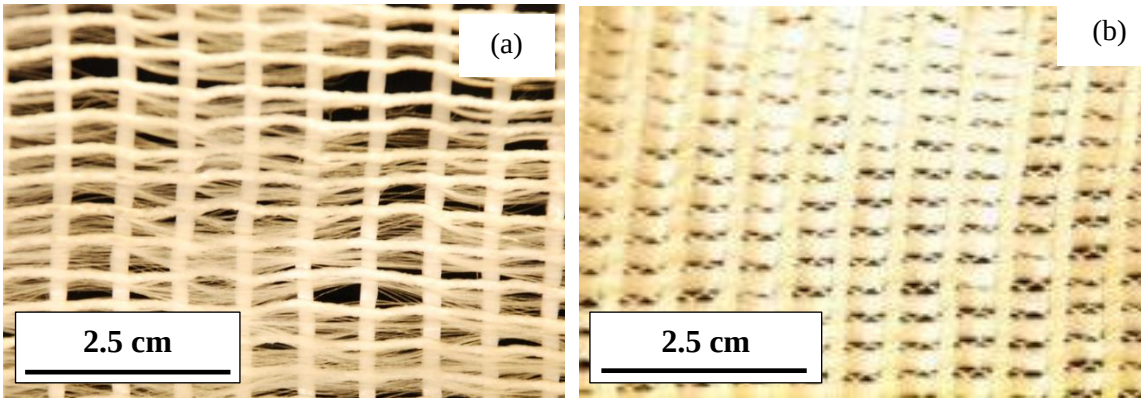

Figure 40. (a) Open weave and (b) tricot weave patterns of textiles woven from MF40.

4.2 Experimental Program

Mechanical properties of the newly developed textile reinforced composites (TRC) were compared to the filament wound unidirectional continuous fiber composites studied earlier in chapter 2, as identical dosages and mixture composition The three different TRC specimen groups studied are shown in Table 8. Three sets of TRC laminate sections (30x6x0.5 in) were cast in the preliminary study of the textile materials with the two different weave patterns mentioned above. Direct tension tests were conducted on TRC coupons (12x2.25x0.5in.) after 7 and 28 days of curing.

Table 8. Groups of specimens of TRC developed in the study

Group ID	Yarn Type	Textile Weave	Yarn V_f%	Matrix Composition
I	MF40	Open	4.0	Control
II	MF 40	Tricot	4.0	Control
III	MF 40	Open	8.0	Control

4.3 Specimen Production

The use of automated pultrusion system enables casting of textile reinforced concrete laminates of desired geometry and layout with desired consistency, accuracy, and speed. The main input variables in this system are the specimen geometry, mix design of the cementitious matrix, type and dosage of fabric, and amount and duration of the applied pressure while casting. While the pultrusion process is automated, certain manual efforts are necessary during the manufacturing process. This includes handling of the pultruded section and surface finishing of intermediate and final layers of laminate, to ensure a uniform and smooth composite surface. The automated pultrusion system for manufacturing TRC was used for manufacturing TRC plates from which coupons were harvested in the desired dimensions.

4.4 Mix Design

A water to cement ratio of 0.32 and cement to sand ratio of 2:1 were used for all samples. 5% of the cement was substituted with silica fume and 10% was replaced with wollastonite for a total cement substitution of 15%. Superplasticizer was used to increase the workability of the mix, specifically for the paste bath to allow for better coating of the textile. Standard laboratory mixing procedures were followed as a fixed, 5L Hobart mixer

was used to dry mix materials for one minute, followed by four minutes of wet mixing. A high range water reducer and a retarder were used to ensure a consistent rheology of the cement matrix The basic mix design used in this study is summarized in Table 9.

Table 9. Mix Design of TRC specimens

Material	Weight Percentage
Portland Cement (Type III/IV)	46.75%
Silica Fume	2.75%
Fine Silica Sand	27.5%
Water	17.5%
Wollastonite	5.5%
Superplasticizer	0.01%

4.5 Results and Discussion

The use of LVDT was again emphasized in the TRC laminate test. The nature of the crosshead stroke and LVDT displacement is shown in figure 41 which helps characterize specimen behavior accurately but only till a certain time in the test due to its small range.

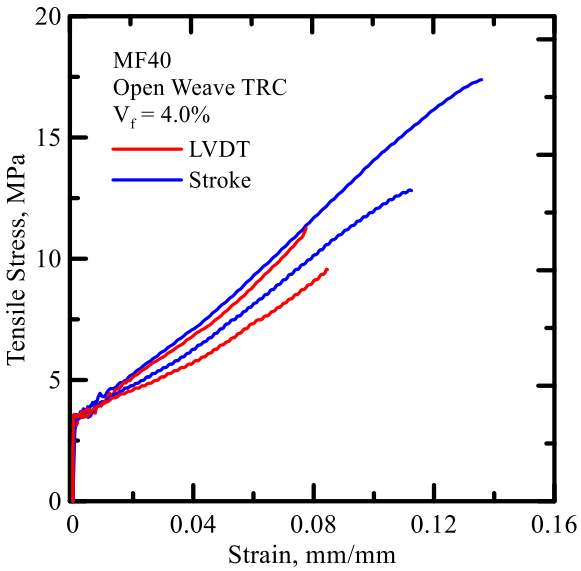

Figure 41. Stroke versus LVDT response for MF40 TRC laminate.

The LVDT response is used in estimation of initial critical parameters like first cracking strain and stress, elastic modulus, post peak modulus. The overall composite parameters like toughness are measured using stroke displacement data.

4.5.1 Comparison of TRC with Unidirectional MF40 tension response

The stress strain response for TRC in tension is similar to the tensile response as shown in figure 33 of chapter 2 with the main 3 stages of elastic behavior till first crack, multiple cracking and delamination followed by crack saturation and pullout of textile reinforcement. The warp yarns prolong the multiple cracking phenomena and several fine closely spaced cracks are formed. These cracks then start merging into each other specimen reaches its full capacity. The structural degradation of the system thus is slow and cracks do not widen as unidirectional fiber laminates giving TRC a higher durability.

Figure 42 shows images of TRC samples at 500 seconds in tension. The MF40 laminate shows multiple fine cracks which have not reached saturation. Thus displaying wider multiple cracking zone. The open weave TRC samples, on the other hand show wider cracks. Despite the volume fraction being 4% for the unidirectional and TRC laminate, in the TRC system, only half of the volume fraction is contributing to the mechanical response in tension. The weave thus does not provide much stiffness and cracks begin to widen. Both 4% and 8% samples show fairly similar degradation, with 8% showing a higher post peak stiffness. Similarly, the weave does not contribute much for 4% TRC.

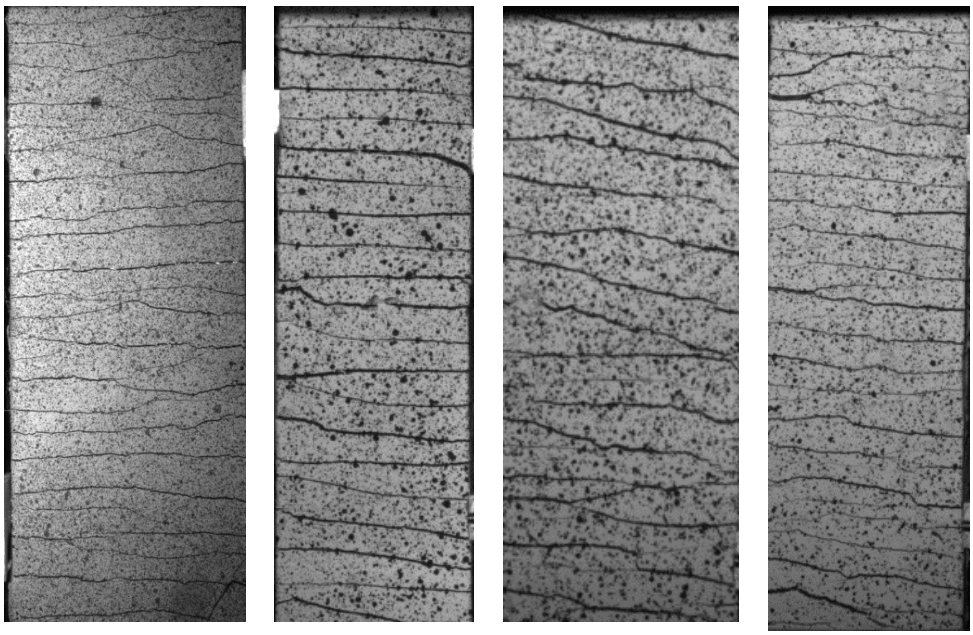

MF40 4%UD laminate | Open Weave 4% TRC | Open Weave 8% TRC | Tricot Weave 4% TRC

Figure 42. Replicate images at 500 seconds tested in tension.

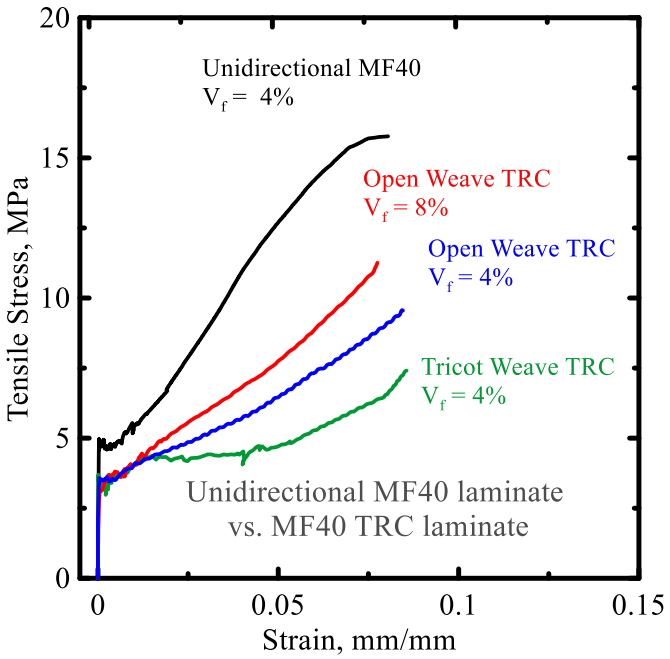

Figure 43. Stress Strain response for TRC data compared with unidirectional MF40

3.4.2 Effect of Textile Volume Fraction

Figure 44 shows replicate plots for stress strain response of open weave samples at 4% and 8% fiber dosage. A clear indication in enhancement of composite stiffness is seen in 8% fiber dosage. Although the ultimate strain capacity is 8% for both the sets due to same fiber matrix composition. Toughness and post peak stiffness is increased marginally by 40% in 8% samples than 4%. The initial response of the composite i.e. Stage I is governed by the matrix properties and hence shows similar strengths. Multiple cracking phenomena dominates and helps achieving higher tensile strengths and toughness in 8% textile dosage. The weave interlocking is similar and the next section discusses the effect of the weave on tensile response of TRC.

There isn't a clear demarcation of when multiple cracking ends and delamination followed by pullout is reached. The cracks being fine show smoother response in the multiple cracking zone. 4% TRC although shows bigger cracks than 8% in the initial strain range up to 1% strain development.

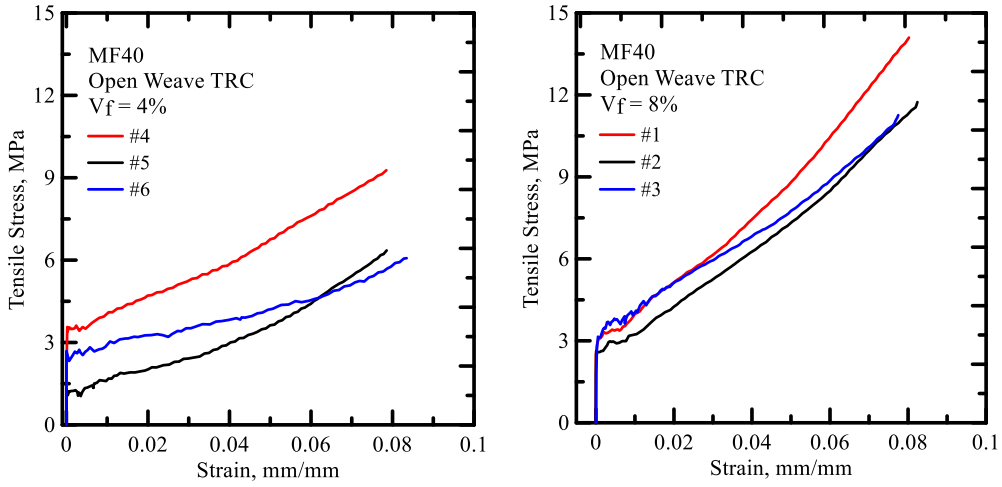

Figure 44.Tensile Stress Strain Response of MF 40 Open weave TRC at (a) 4% dosage. and (b) 8% dosage of textile in a control mix.

4.5.2 Effect of Weave Pattern of Textiles

The main difference in the weave pattern in an open weave compared with tricot weave is that for a tricot type of a weave, a higher interlocking and tightness of the textile is achieved. This gives a tighter orthotropic structure to the sample making it stiffer in the transverse direction. The first cracking strength for a tricot weave is 4 MPa whereas it is 2 MPa for an open weave sample. Once the matrix cracks the load is transferred to the fibers and the crack propagates through the width of the laminate. This propagation is slower due to the tightness of the weave and availability of warp yarns to distribute force back into the surrounding matrix. Thus, a higher first cracking strength is observed for a tricot weave TRC laminate.

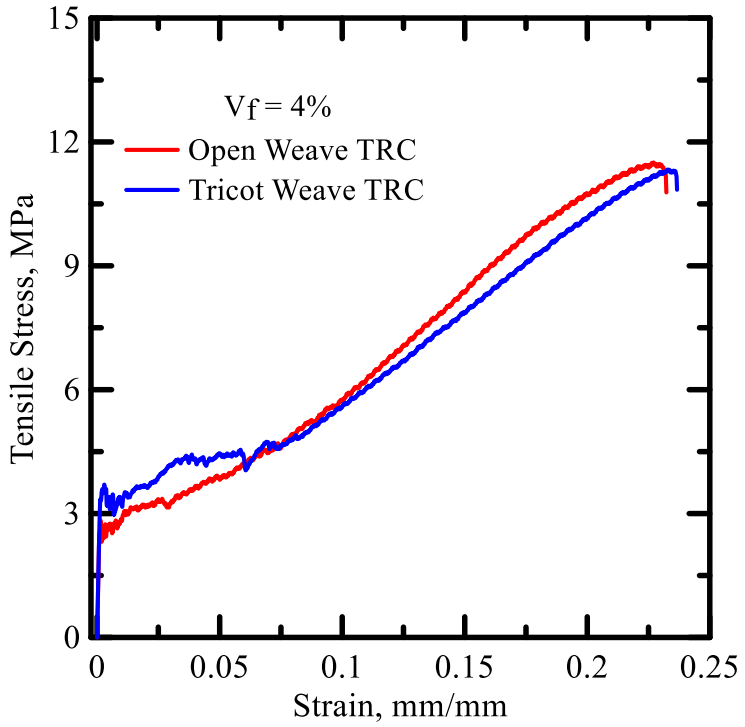

Figure 45. Effect of weave pattern in TRC stress strain(stroke) response

. The multiple cracking is fairly similar with a tougher range for tricot weave. The strain hardening in both the weave patterns is similar with a close post peak stiffness due to the volume fraction of textile being the same.

4.7 Conclusions

Damage in such woven textile reinforced systems accumulates due to failure in the transverse direction. Multiple cracking is dominant mode of failure. The mechanical properties thus depend on fiber type, weave pattern and matrix formulations. Accumulation of cracks reduces the post crack strength gradually compared to a stiffer unidirectional system. A stabilized crack pattern remains over a strain range after multiple cracks and formed and widening of cracks takes place. This contributes to a higher toughness of the composite thus giving a ductile composite system.

5.APPLICATION OF DIGITAL IMAGE CORRELATION FOR DAMAGE EVALUATION OF COMPOSITES

5.1 Introduction

Digital Image Correlation has been a widely accepted, reliable and robust non contacting method of measuring deformation in the field of experimental mechanics. The set up used in early 1980s is shown in the schematic Fig.46.The test set up has fairly remained the same over the years, with advancement in cameras.

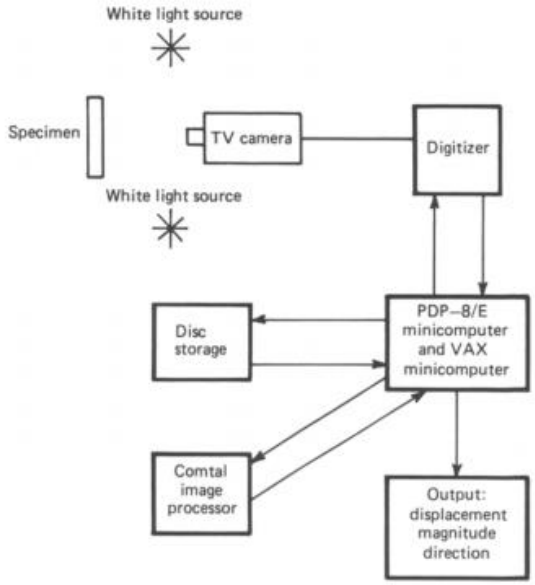

Figure 46. Experimental configuration for correlation analysis.

5.2. DIC Data Acquisition System

DIC requires the following equipment and specimen preparation to record the test data. High resolution cameras capturing the specimen area of interest. A light source which illuminates the specimen uniformly. The specimen needs to be prepared in the following fashion with random greyscale speckles marked on it. Fig. 47 shows the DIC set up available in the Structures lab at Arizona State University. Figure shows how DIC data is correlated with the experimental test data.

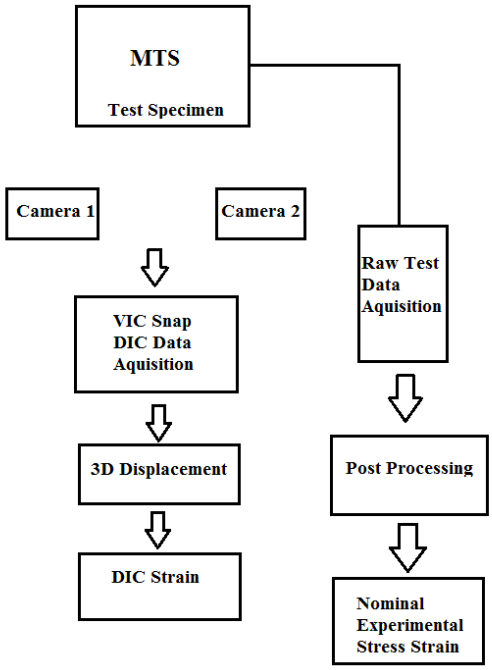

Figure 47.Flowchart explaining DIC correlation with experimental data.

5.3 DIC Terminology

- Area of Interest:

The subset and step size can be selected after an area of interest (AOI) is created. DIC is essentially a displacement measuring tool which tracks the same physical points as shown in the original image over a given area of interest (AoI). Figure shows the area of interest marked on a tension composite.

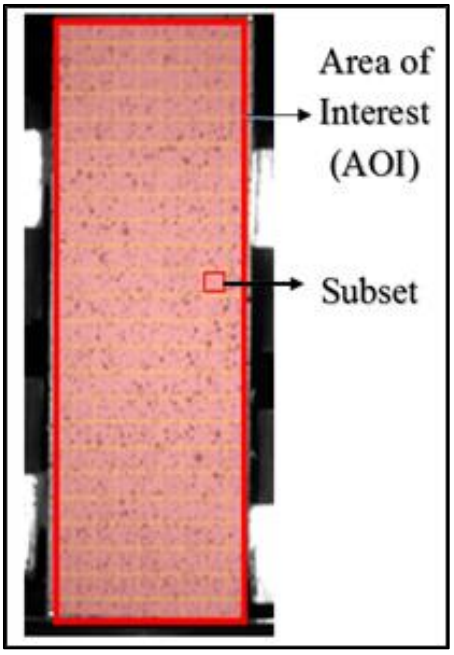

Area of Interest and subset

- Speckle Pattern:

To perform DIC, a random contrast speckle pattern is required over the area of interest which estimates the displacements by tracking the movement over consecutive images. Digital image correlation requires that the specimen is properly and densely speckled. Each subset throughout the speckle pattern should have unique information within it. A pattern with uniformly sized subsets, 50% coverage of speckles of high contrast will result in accurate cross correlation and yield the most traceable features by reducing the noise levels in the data.

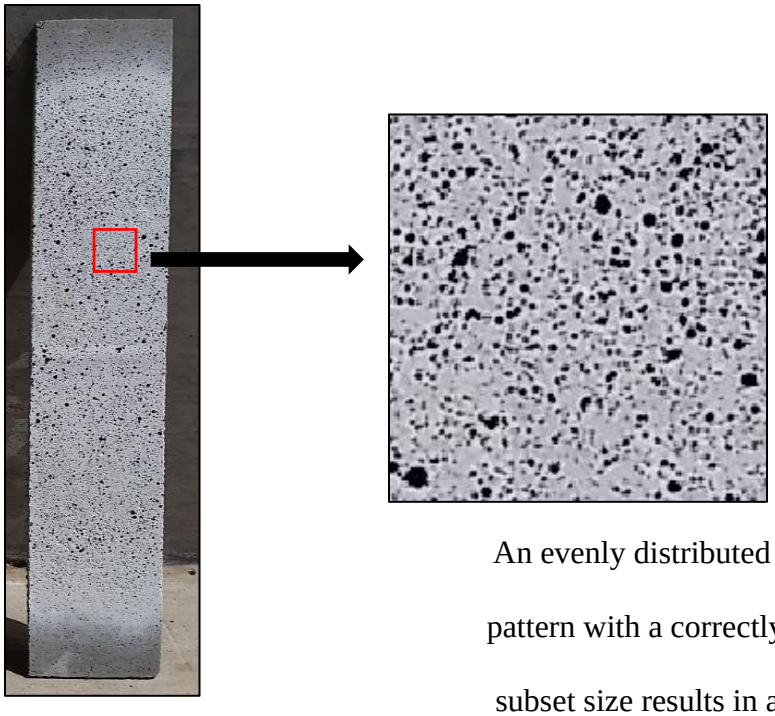

An evenly distributed speckle pattern with a correctly chosen subset size results in accurate

Speckle pattern on a finished DIC laminate

- Subset Size:

The subset size controls the area of the image that is used to track the displacement between images. It should be large enough to ensure that there is a sufficiently distinctive pattern contained in the area used for correlation. The subset and step size can be selected after an area of interest (AOI) is created. VIC 3D- 7 provides an initial guess of the subset size by reading the speckle pattern. A general rule of thumb to select a subset size follows that every subset much includes fairly 50% speckle and a high contrast for accurate correlation.

- Step Size

The step size controls the spacing of the points that are analyzed during correlation. If a step size of 1 is chosen, a correlation analysis is performed at every pixel inside the area-of-interest. A step size of 2 means that a correlation will be carried out at every other pixel in both the horizontal and vertical direction, etc. Thus, a smaller step size increases the

computational time and cost. However, using a smaller step size can help detect fine cracking as it considers every pixel over the subset.

The following image shows the same crack analyzed with a step size of 2 and 7 respectively. The crack width and spacing measurements thus can be accurate with a smaller step size but more expensive and time consuming.

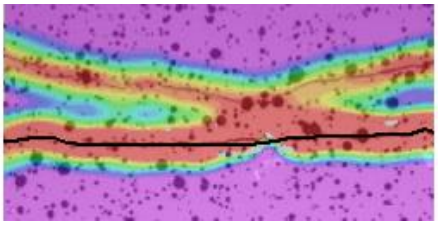

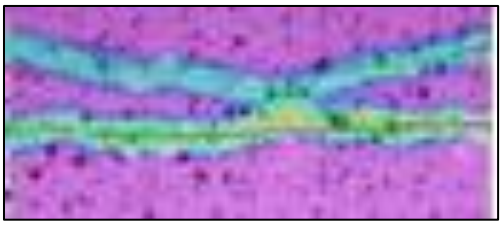

5.4 DIC Analysis using VIC 3D- 7

Tension test is run on the sample and distributed cracking is studied using digital image correlation. This section encompasses the general procedure adopted to run the analysis on a sample and deals with tackling issues faced in the process. Several factors such as inherent sample defects, irregular speckling pattern, warped or uneven sample geometry, low resolution images etc. causing a lot of noise in the data which yields incoherent results.

VIC 3D Interface has the following view.

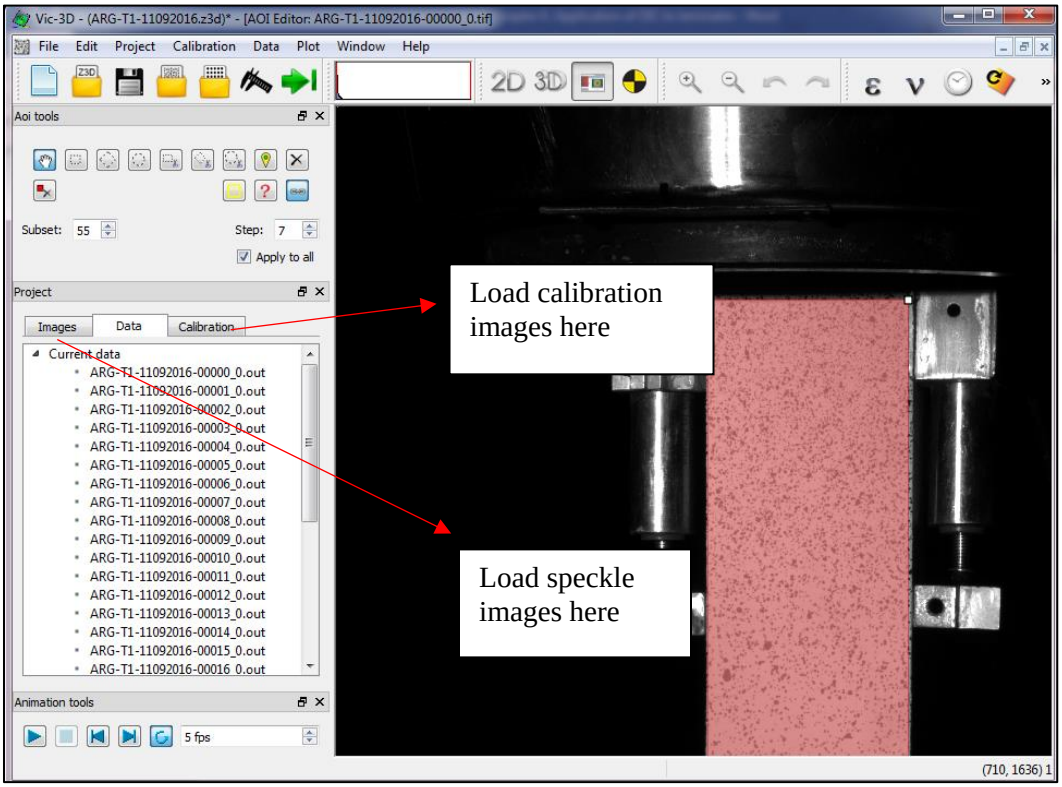

5.4.1 VIC 3D-7 Analysis - Step by Step Procedure

Add speckle images in the Images tab under current project.

1. Choose range of speckled images to be analyzed. (Starting point to the final point till where the sample needs to be analyzed for cracks.
2. Calibrate the images by either adding the calibration file or manually calibrating based on the sample dimensions.
3. Select area of interest within the sample.
4. Using the initial guess select the subset size and step size for the test.
5. Run the test by clicking on the green arrow. You can select every speckle image or reduce the size by analyzing only some of them by checking the options mentioned.

6. Once the test is run, using inspector tools, draw a straight vertical line at the middle of the sample and extract the eyy Lagrange strain values in the format as seen in the following images.
7. Details about the procedure and problems faced during DIC are addressed further.

Once, the speckle images are added and the reference image is chosen (start point of the test), the area of interest is selected and subset size and step size is defined. To run the displacement analysis, select the *Run Correlation* entry from the data menu. The deformed images to use for correlation analysis can be selected from the list box on the dialog. Selected images are indicated by a check mark. Above the list box, buttons are available to select/deselect all image files contained in the list box. To select 1 data file from every 2, 5, 10, or n, right-click in the file list and choose the desired option.

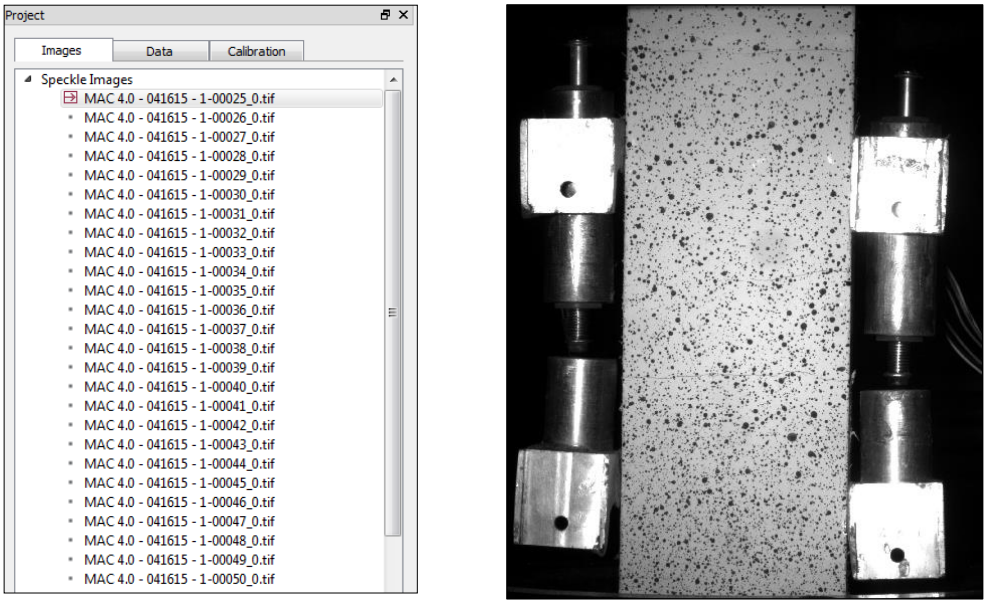

Figure 48. Reference Image with distinct speckle pattern:

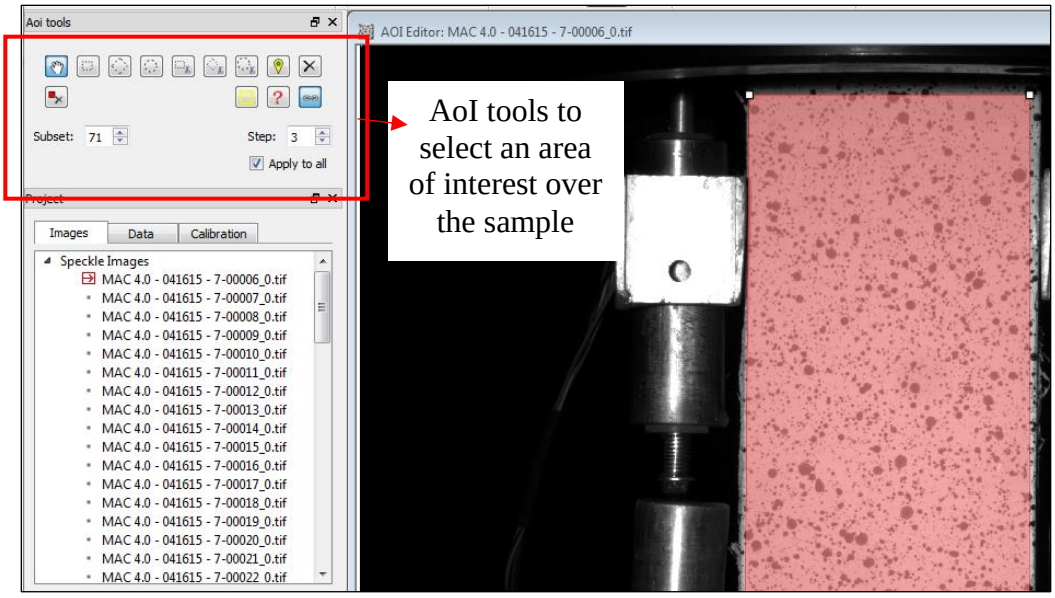

Figure 49. Snapshot of VIC 3d-7 interface for step 1 through 3

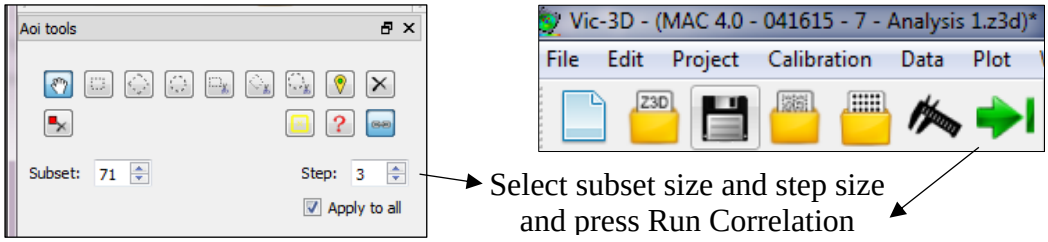

Figure 50. Snapshot of VIC 3d-7 interface for step 4 and 5

The correlation runs for every image loaded in the speckle images tab and calculates the displacements and strains sequentially using cross correlation or normalized correlation algorithms. Figure 43 shows the tabs in VIC 3D-7 which help in customizing the displacement and strain outputs as required. The Post Processing tab contains the strain tensor data which can be modified for every type of test.

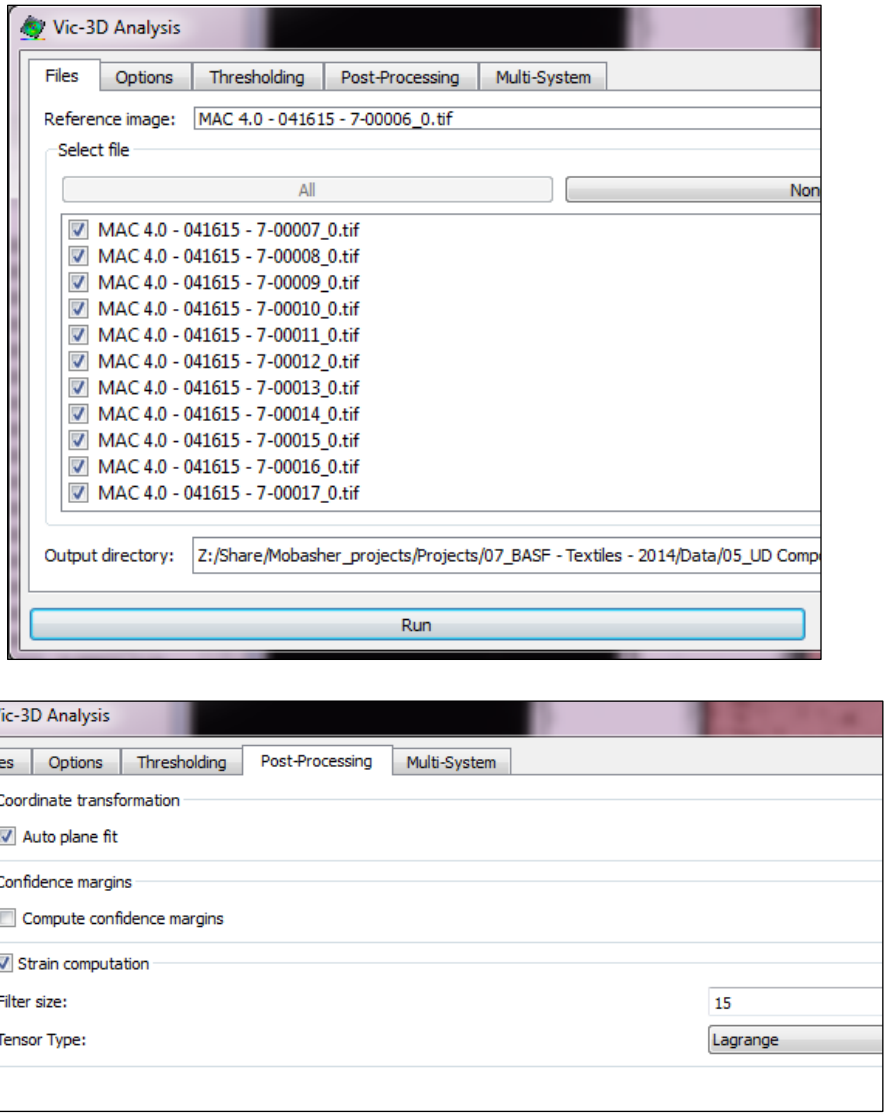

Figure 51. Select the images to analyze and strains to compute using post processing tab.

Next Step is data extraction from the correlated analysis in the data tab. The contours required for quantifying tensile properties are the Lagrangian strain in yy direction which is the direction in which the sample is pulled. Locations where cracks form show contours as shown in figure 44. A straight vertical line is drawn along the sample in the Y direction and the V displacement along this line are obtained. This forms the basis for post processing of the DIC data.

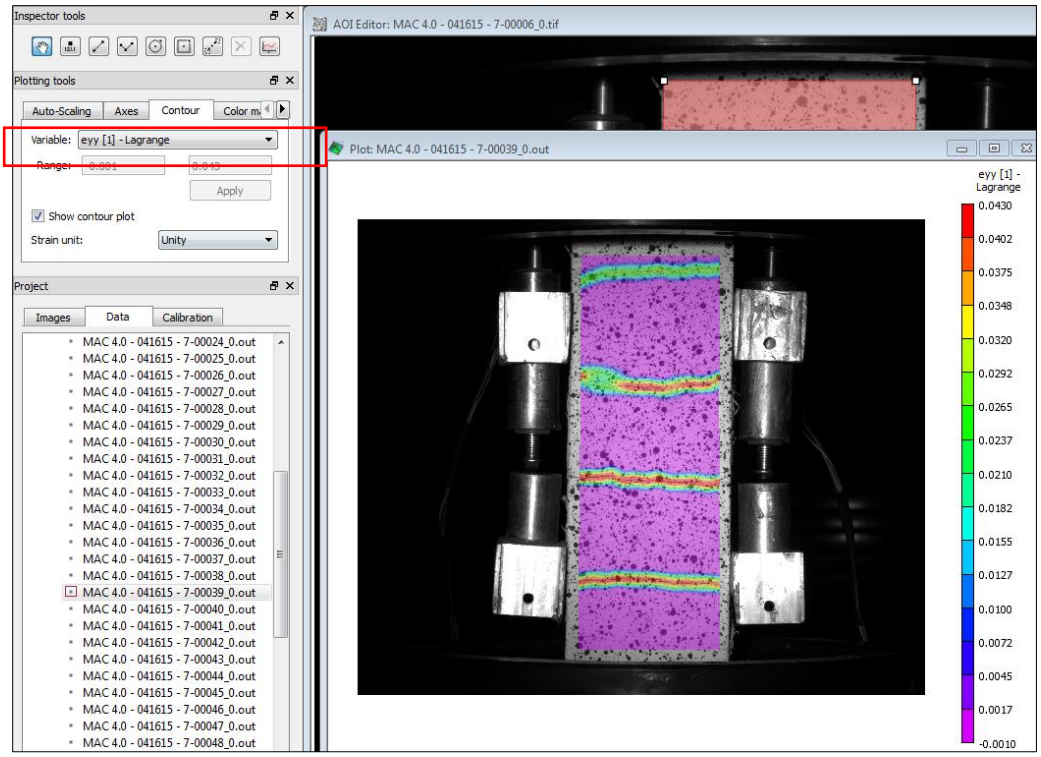

Figure 52. DIC results post analysis, inspector tools to be used to retrieve contours for all test images.

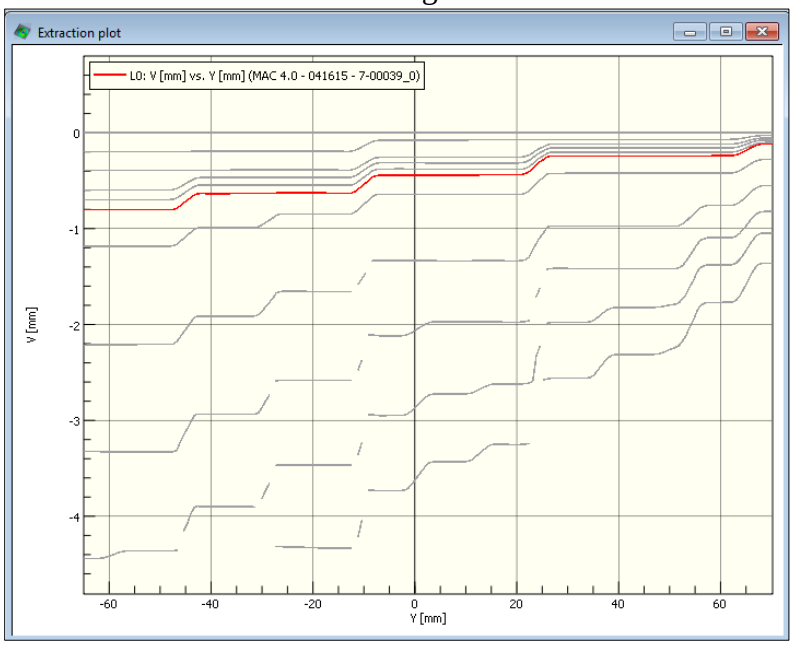

Figure 53. V vs. Y field for MAC 4% unidirectional laminate

This data can be extracted for post processing, displacement field V along Y length of the specimen. Highlighted field represents current image selected showing 4 cracks as shown in figure 45.

5.4.2 Post Processing of DIC Data for Damage Evaluation

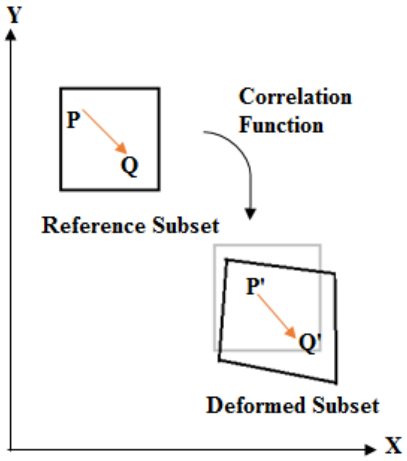

Figure 54. Schematic which cross correlates the position vector PQ over a specific

The corresponding deformed subset is found by searching for the subset that renders the correlation coefficient maximum or minimum in the deformed image. By this means, the point in the deformed subset is located and the strain over the AoI is derived by taking the gradient of the displacement field. VIC 3D-7, commercial software developed by Correlated Solutions, Inc was used to run the DIC analysis for the tensile tests on laminates. The DIC technique was further used for automated determination of crack density, crack spacing, and characterizing damage evolution as the test progresses. Evolution of distributed cracking mechanism and local strain fields can be easily documented as shown in figure 55.

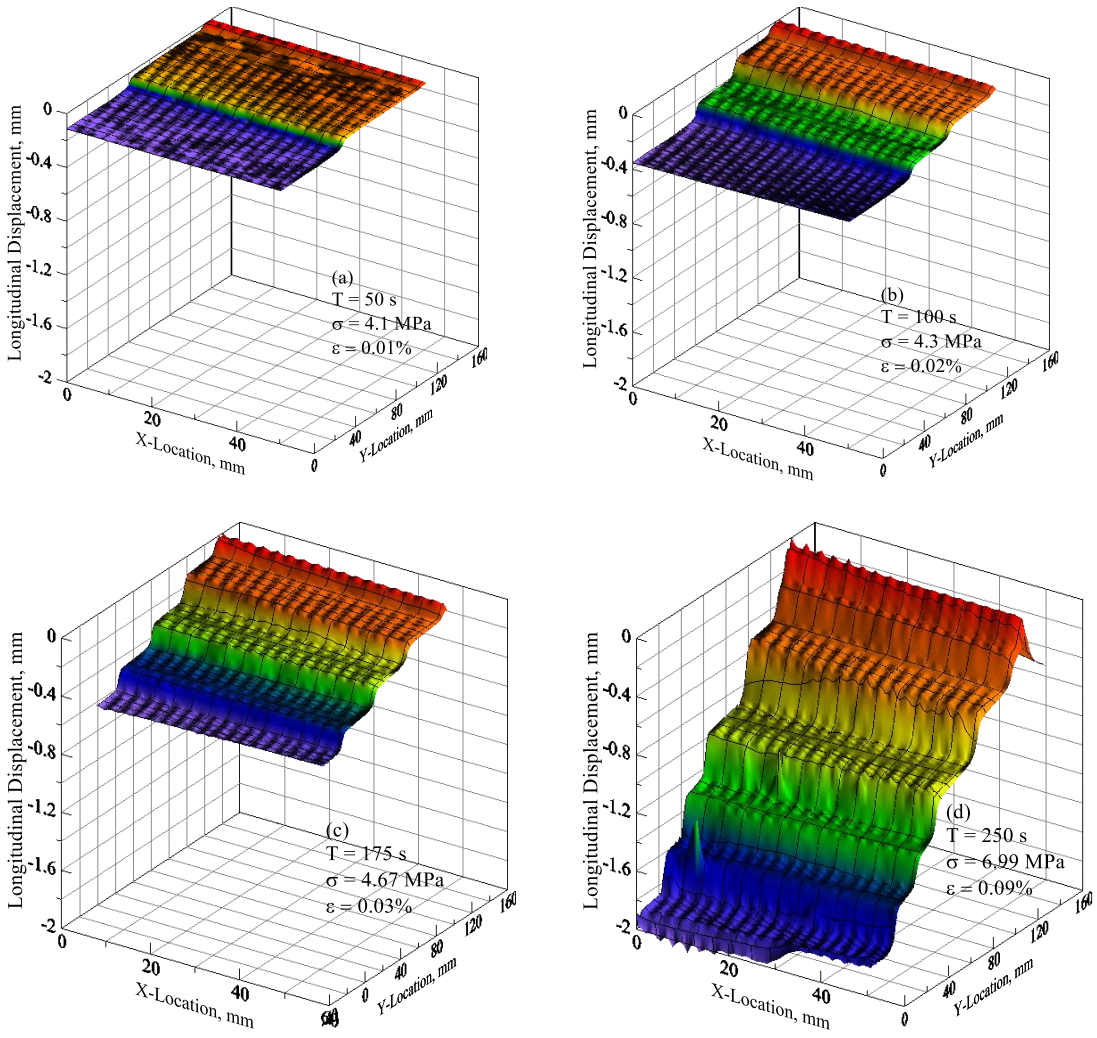

Figure 55. 3D displacement field of filament wound composite with MAC 2200CB at 4% dosage in tension.

5.5 Damage Characterization of Parallel Cracking Behavior in Laminates

5.5.1 Crack Width and Spacing Estimation

The DIC images serve as the input for deducing the crack width and crack spacing parameters for the specimen. Each crack width is tracked with from development stage to saturation stage with time. Data extracted from DIC analysis is shown in Figure 56 (a) and (b) shows the contour of longitudinal V displacement versus Y location for a MAC 4% (replicate 1), when all the cracks are formed. Each crack is demarcated as the discontinuity

in displacement field V along the Y location of the sample as shown in the figure. A certain crack width is measured by the V displacement of this step as shown and the crack spacing is marked as the distance Y between two cracks as shown in Fig 59 (c) below.

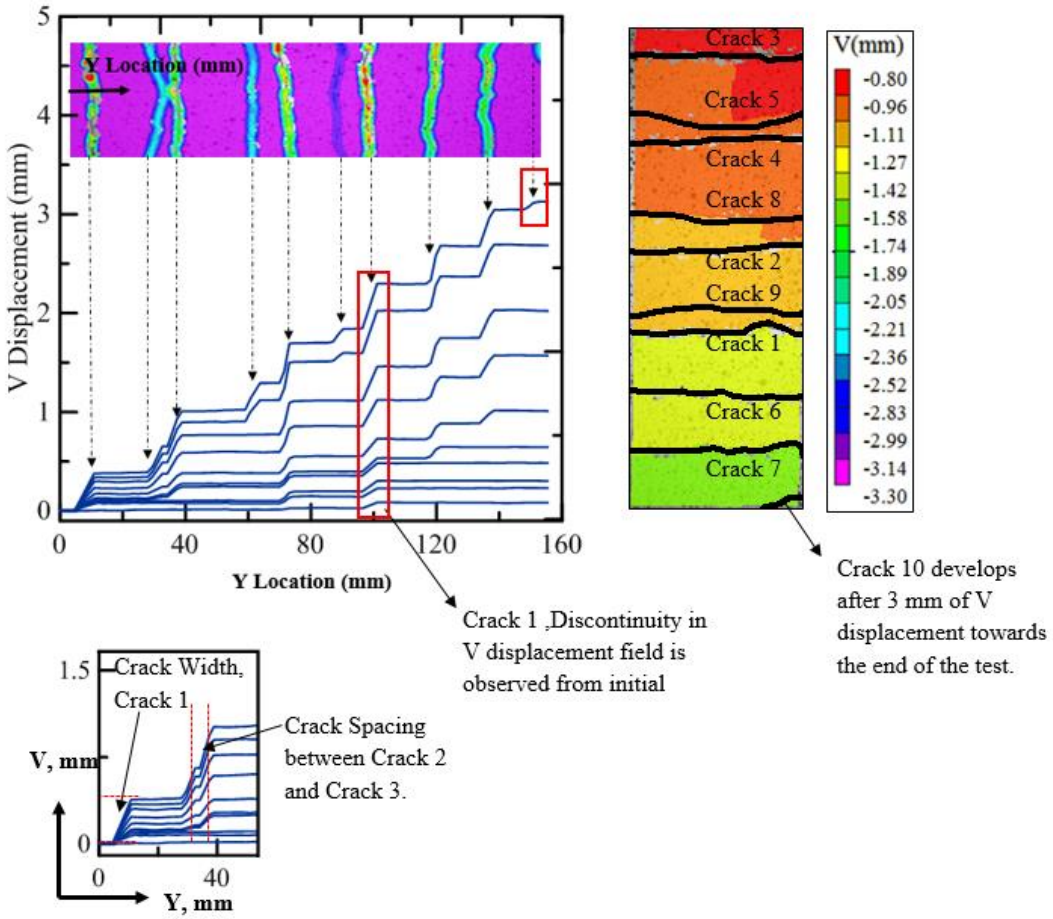

Figure 56 (a) Distribution of longitudinal strain is reported at distinct time steps, (b) DIC V displacement contour showing multiple crack formation at saturation stage, (c) Crack Width and crack spacing estimation.

A total of 9 distributed cracks propagated throughout the width are observed. This data is then post processed in a MATLAB code to generate the crack width and spacing response of the sample until failure. Figure 10 shows the response generated with time. Experimental stress vs. time is compared with the crack occurrence with time. The

experimental stress vs. time history for the sample is compared with individual crack openings estimated by DIC post processing. Figure 57 shows the response.

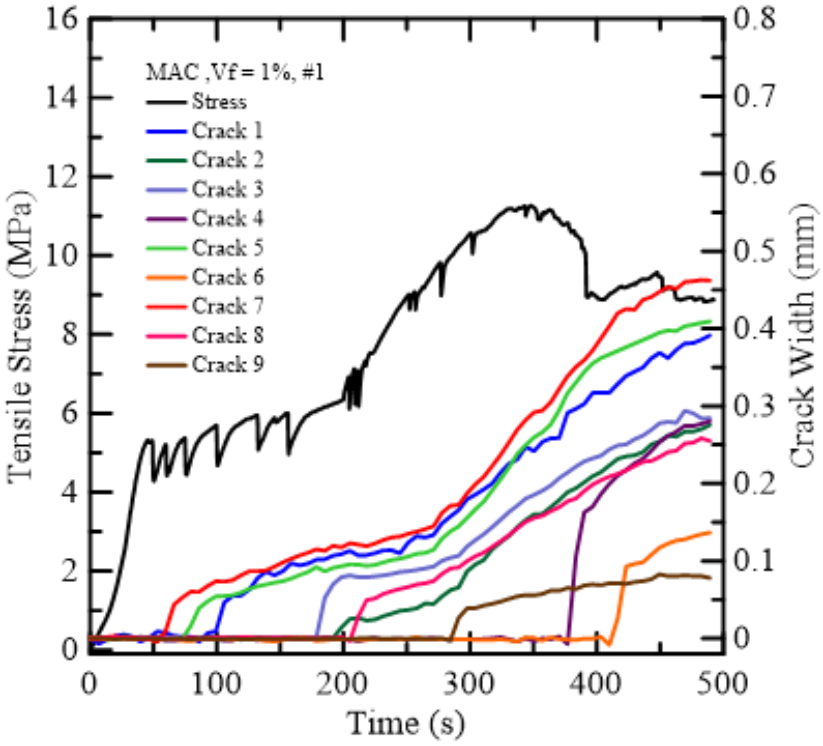

Figure 57. Time history of stress and crack width development for MAC 4%, #1.

Crack 1, 5 and 3 develop early on, between the first 100 seconds in the test, widen further within the time range of 250 to 400 seconds and achieve a high crack width opening of 0.4 mm towards the end of the test. However, Crack 6 and 9 open after the sample has reached its maximum stress capacity and the remaining cracks have reached a saturation crack width. The development of new cracks when sample approaches maximum stress indicates that multiple cracking stage of the overall composite is ending and the sample response is approaching saturation stage. The crack spacing is stable at this point and sample is in the last stage of crack widening leading to failure by fiber pullout. The crack spacing is measure as the distance between two cracks as marked on the contour. At every strain, the number of cracks and their individual spacing is measured. The mean crack

spacing from these values indicates the damage induced at that point. As the strain increases, the average crack spacing reduces and reaches a saturation crack spacing. Figure 58 shows a saturation crack spacing of 20 mm at 0.015 strain.

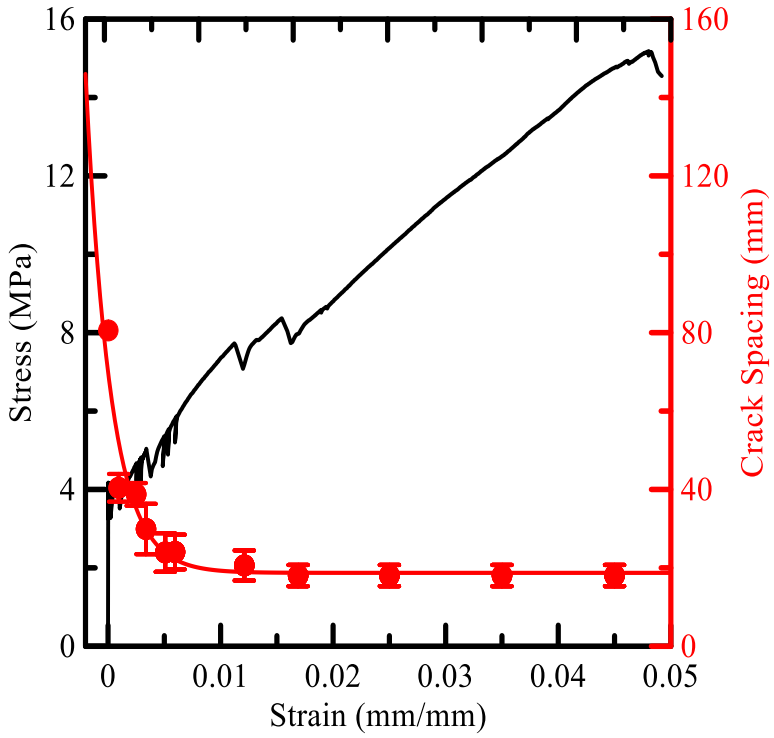

Figure 58. Tensile stress-strain, and crack spacing response of MAC 4%, #1.

5.5.2 Strain Correlation using DIC Displacement

The displacement measured using DIC was compared with the traditional method of LVDT mounted directly on the specimen. It is to be noted two LVDT with deformation measurement capacity of up to 8 mm were mounted on the specimen at the middle of the gage length as shown in Figure59. The DIC displacement along two horizontal segments was extracted, such that the differential DIC displacement lies along the points where the LVDT 1 and 2 displacements are measured. Both the mean LVDT displacement and DIC displacement correlate closely which validates the non-contacting DIC method of data acquisition superior to a contact based system

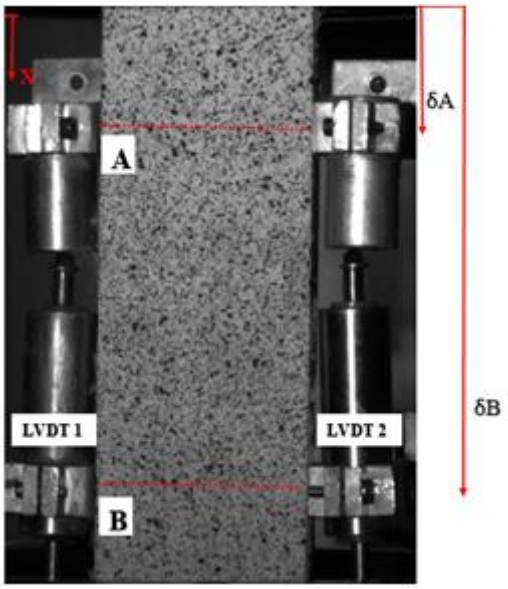

Figure 59. Sample showing LVDT gage length and relative displacement when pulled in tension.

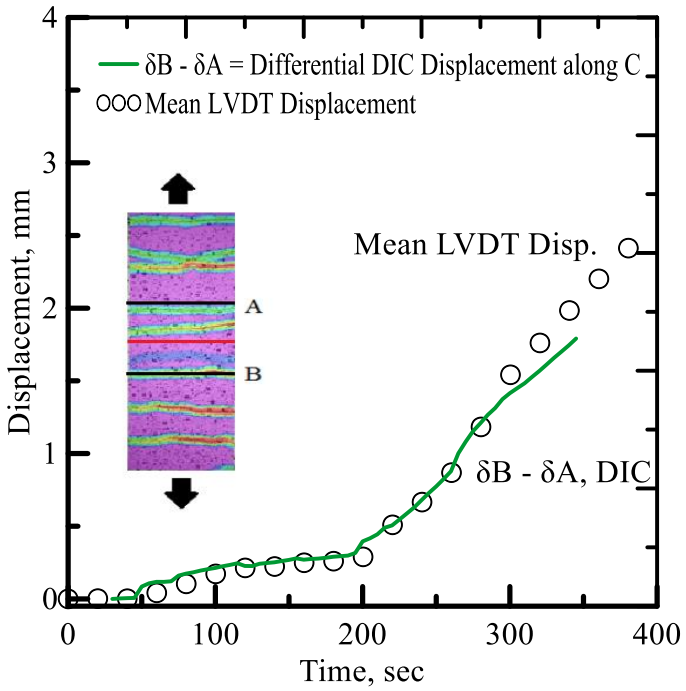

Figure 60. Displacement with Time response for LVDT and DIC

5.6 Results and Discussion

5.6.1 DIC Contours for Unidirectional PP laminates

Multiple cracking is documented for each representative volume fraction of MAC and MF40 samples. This data is quantified using crack width and spacing functions as explained in section 5.5.1. Using the crack density parameters damage can be further characterized and stress strain response can be simulated.

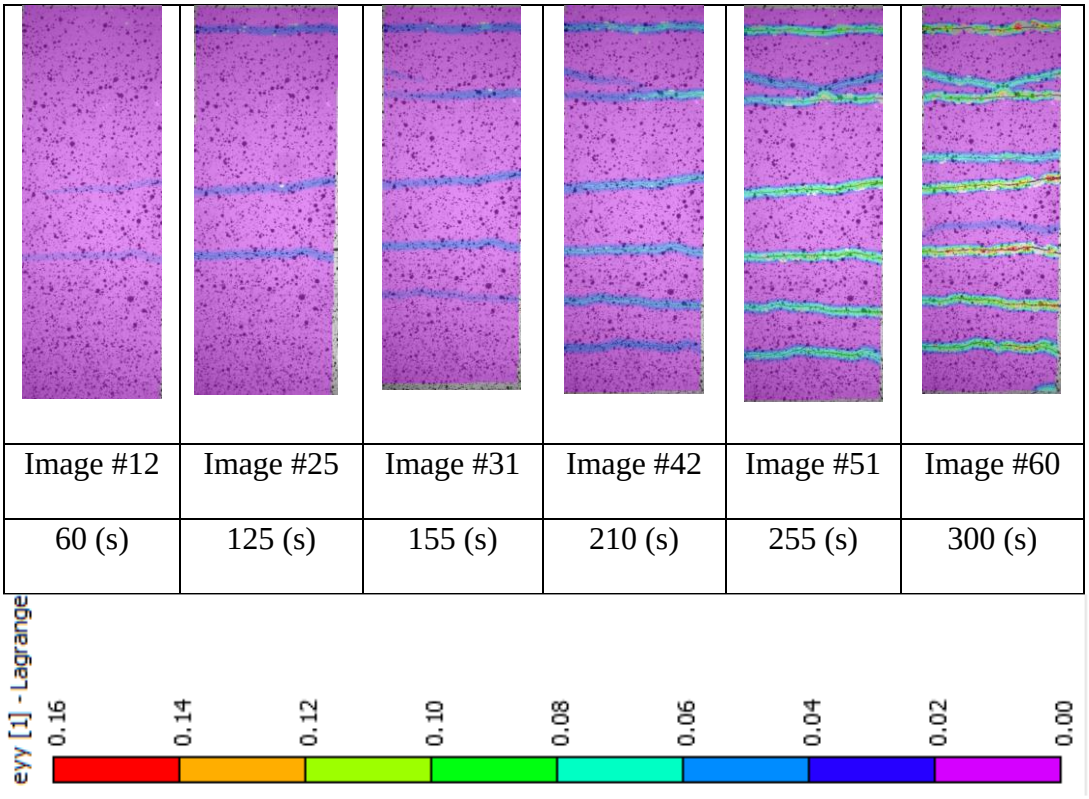

Figure 61. DIC eyy strain contours showing multiple cracking.

Figure 62 shows the 3 representative curves for MAC samples with control mix for 3 different fiber dosages. It should be noted that the crack spacing value is an average value and as multiple cracks form the average crack spacing decreases exponentially till it reaches a crack saturation value. This kind of damage function can be fitted to predict the

stress strain response using a laminate composite model. This is the future plan of study for this chapter.

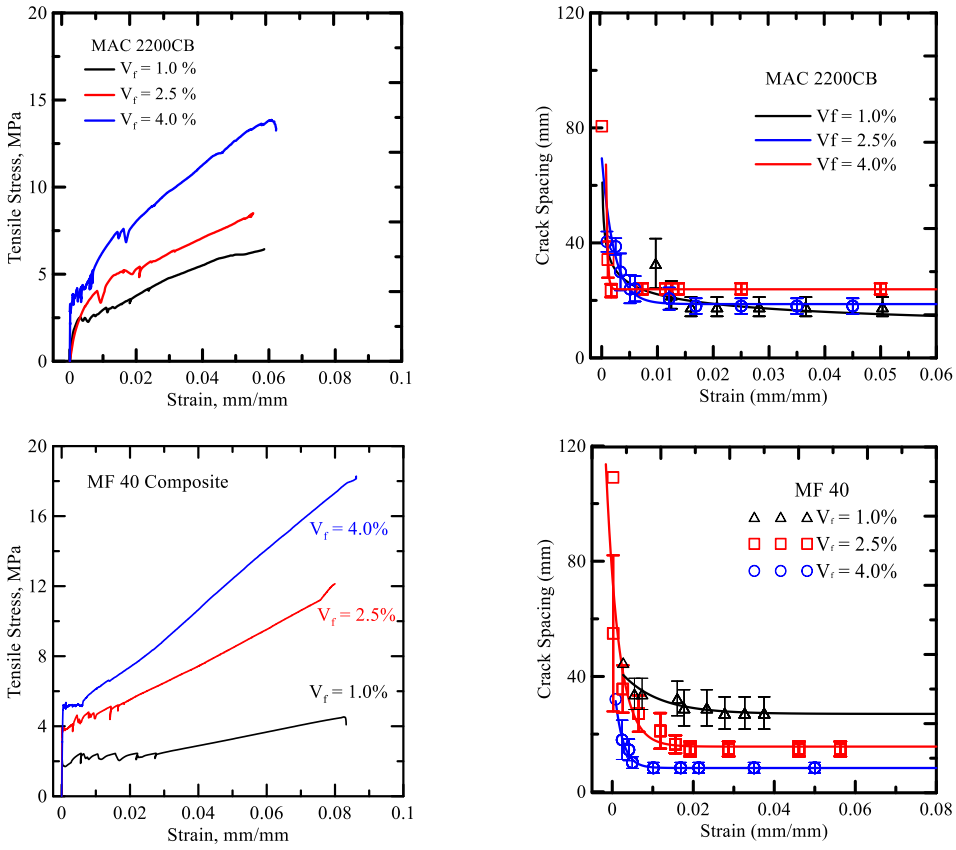

Figure 62. Stress Strain response compared with crack spacing strain response for MAC and MF40 unidirectional laminates.

Stiffness degradation in the post crack correlated with the reduction of crack spacing. Saturated crack spacing, Characteristic Damage State, CDS is defined as a point when there is stress transfer sufficient to induce additional cracking. CDS is a function of the bond of the fiber and matrix.

Stiffness in the post crack region correlated with fiber content as clearly seen in composites with 4% MAC and MF40.

5.6.2 DIC Contours for Textile Reinforced Composites

Distributed cracking mechanism observed in these TRC specimens can be observed using the DIC technique discussed earlier. Strain contours along the loading direction of TRC specimens made with MF 40- open weave fabrics at dosage of 4% and 8% are shown in figure 63 and 64. As evident from the images at the same strain values, multiple cracking dominates the failure. The last image in both the series shows multiple cracking. 4% volume fraction specimen has a smaller strain range of multiple cracking compared to an 8% volume fraction specimen. Higher volume fraction of textile provides additional toughness and post crack stiffness. Nevertheless, the strain capacities for both the specimens remains in the same range.

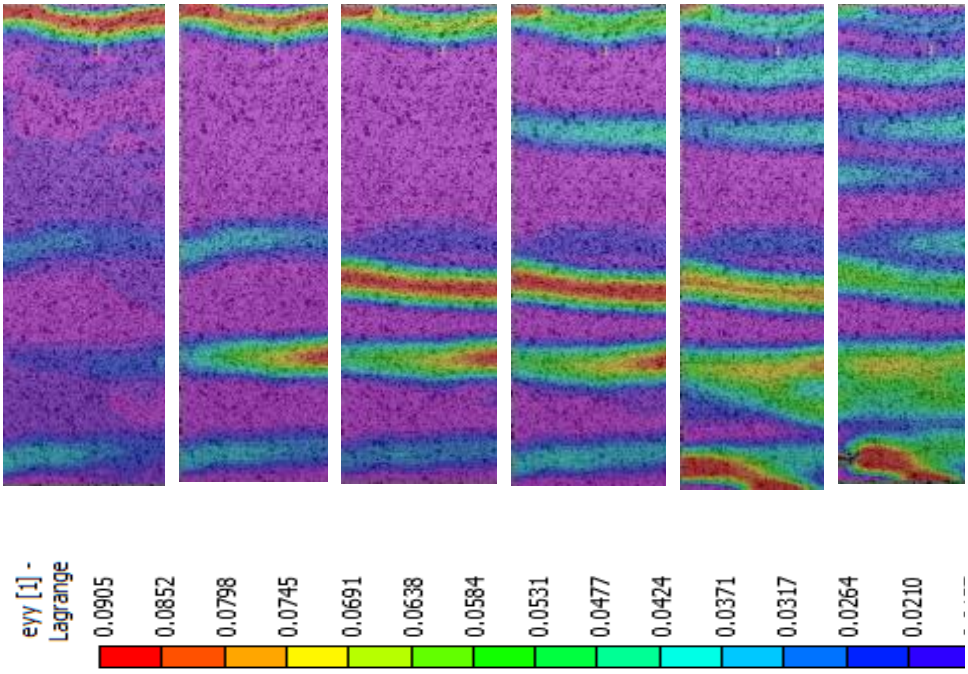

Figure 63. Distributed crack and DIC strain contour observed in representative MF 40 Open weave TRC Specimen at 4% dosage

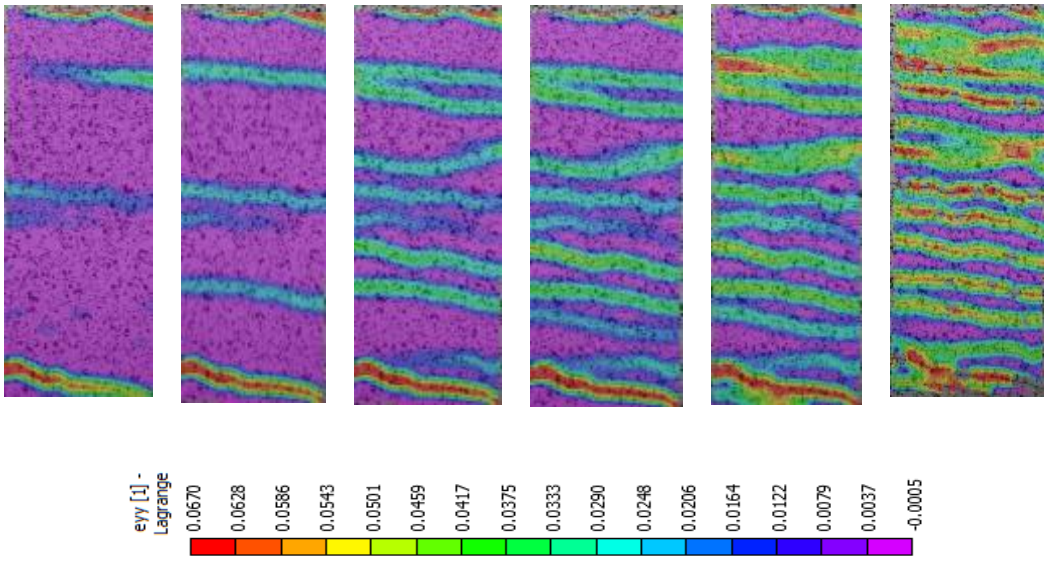

Figure 64. Distributed crack and DIC strain contour observed in representative MF 40 Open weave TRC Specimen at 8% dosage

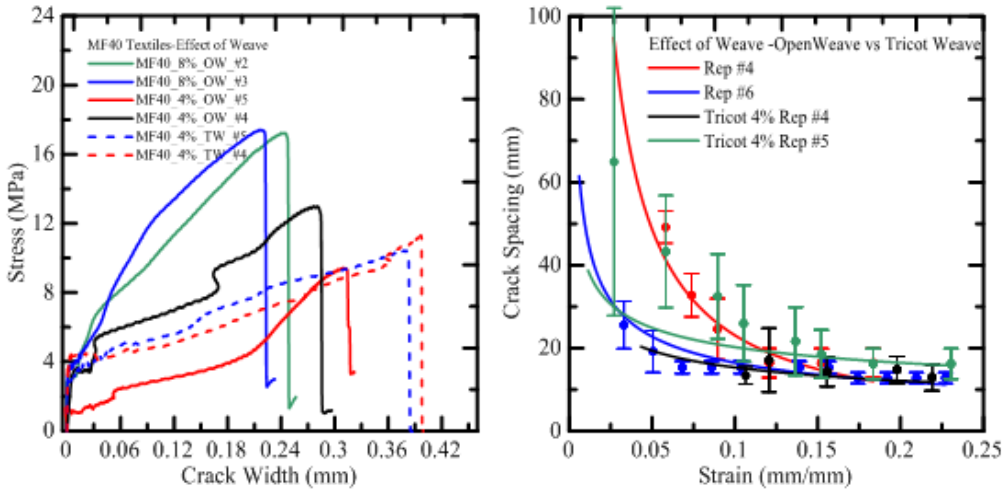

Figure 65.Stress Crack width and strain crack spacing response for 4% open weave and tricot weave TRC.

The stress strain response is compared with the crack spacing -strain response to estimate the stiffness degradation of the TRC composites. It can be observed that tricot weave specimens show a higher crack width at lower stress values whereas, the open weave specimens widen less but reach an average stress range of 8 MPa.

6.FUTURE SCOPE OF WORK

6.1 Development of Structural Shapes

The current work related to the composite response can be applied towards development of new construction products from TRC laminates such as angles, channels, hat sections, closed sections and sandwich sections with optimized cross sections Developing such optimized textile reinforced structural shapes can provide for a robust advanced class of concrete materials in line with light gauge steel sections. The textile reinforcement provides for the necessary tensile reinforcement whereas concrete adheres to the strength and serviceability criteria required form this class of sustainable materials. The proposed structurally efficient and durable sections promise to compete with wood and light gage steel based sections for lightweight construction and panel application. Structural shapes and their viability was studied by the use of digital image correlation to characterize their full scale behavior.

6.2 DIC Results for Structural Shapes

Distributed cracking could be documented using the DIC technique discussed extensively in the previous chapters. The strain development and growth of cracks of a representative 1 m long L-TRC specimen under tension is shown in Figure 58 at different strain levels. Figure 58 shows the lateral strains that develop in a representative 0.6 m long L-TRC specimen under compression.

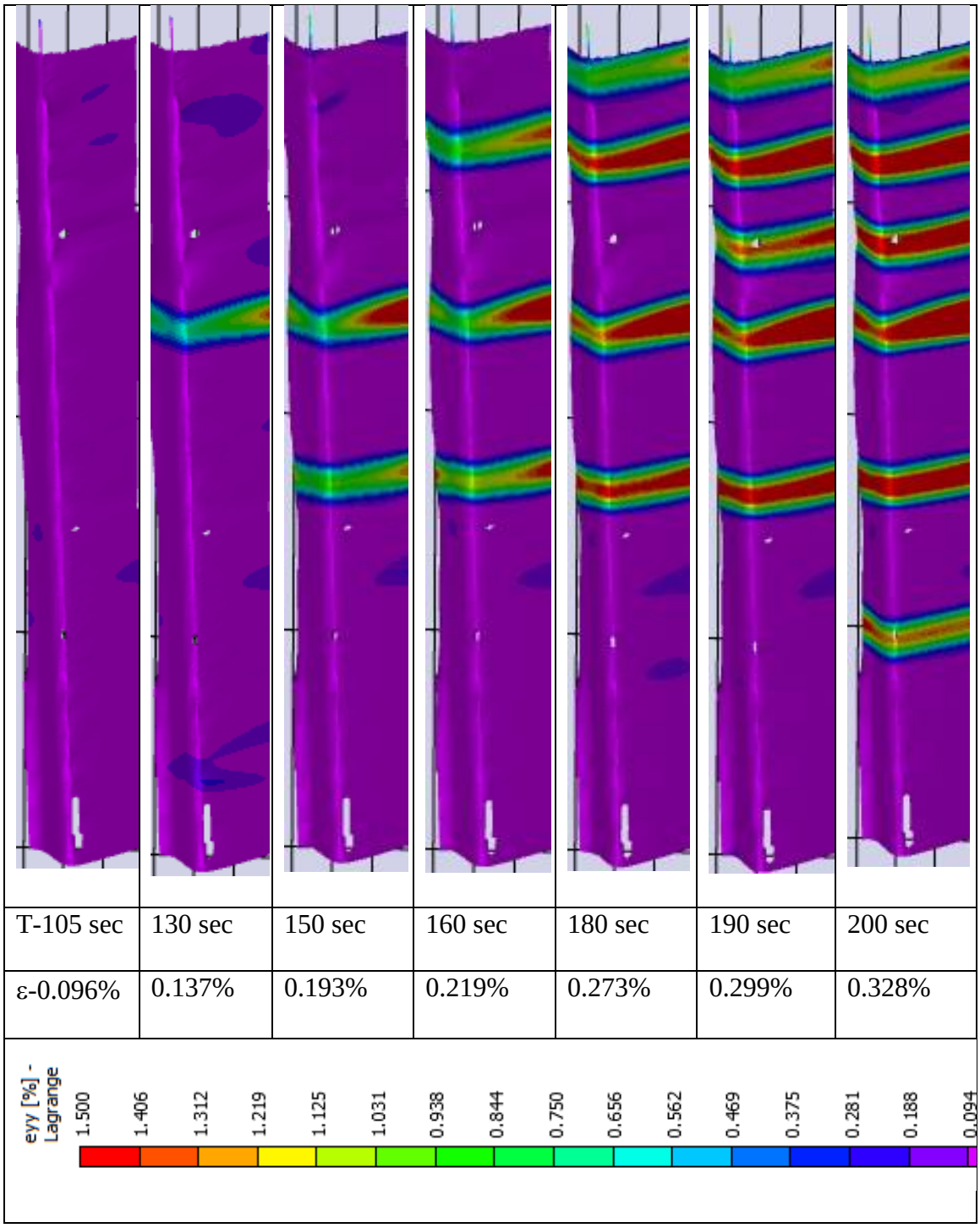

T-105 sec	130 sec	150 sec	160 sec	180 sec	190 sec	200 sec
ε-0.096%	0.137%	0.193%	0.219%	0.273%	0.299%	0.328%

Figure 66. Distributed cracking observed in a 1 m long L-TRC specimen under tension

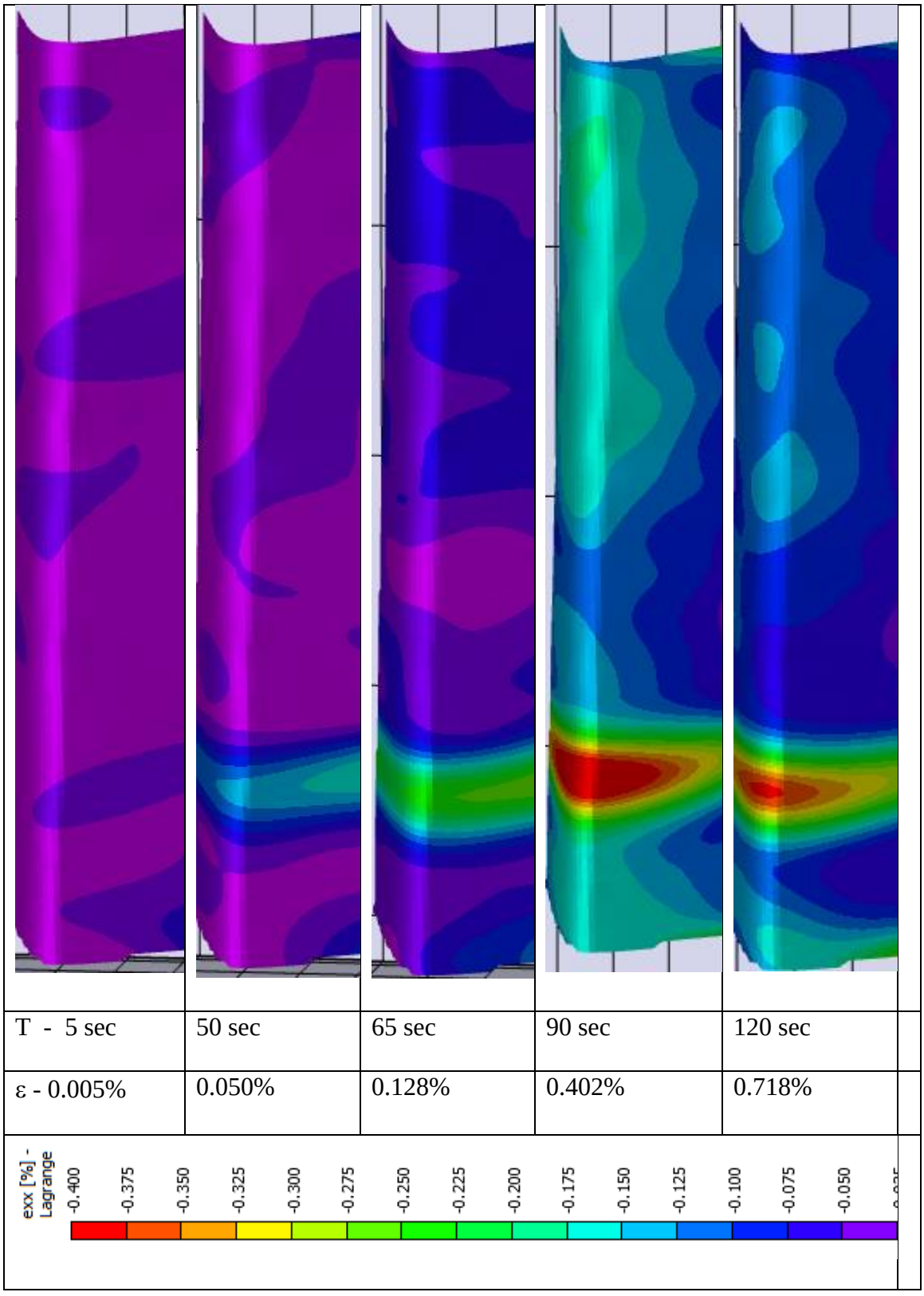

T - 5 sec	50 sec	65 sec	90 sec	120 sec
ε - 0.005%	0.050%	0.128%	0.402%	0.718%

Figure 67. Lateral strains (x-dir) observed in a 1.2m long L-TRC specimen under compression

6.3 Conclusion

Based on digital image correlation one can understand the damage and study its propagation within a volume fraction of fiber composite. DIC proves to be a reliable and scalable method which can capture the complete range of damage in a composite from a few macrostrains to an extent of 8% strain capacity which cannot be measured by a contacting method of deformation measurement.

Additional work in this field can be based upon verification of this damage by evaluating it regarding a damage function and predicting the stress strain response based on composite laminate theory. This predicted response need to be compared with the experimental stress strain response to validate the damage evaluation.

Additional structural shapes like hollow square and circular cross sections, H and I shaped shapes can be manufactured and studied under tension and their damage characterization can be studied to scale the coupon study with varying textile content and comment on their viability. Failure mode of these large-scale shapes and their connection design alternatives can lead the study towards design and development of this new class of material and render its applicability in the construction industry.

REFERENCES

1. Aveston, J., G. A. Cooper, and A. Kelly. "The properties of fiber composites." *Conference proceedings*. Vol. 15. IPC Science and Technology Press Ltd, 1971.

2. Aveston, J. "Single and multiple fracture." *The properties of fiber composites* (1971).

3. Laws, V. "The efficiency of fibrous reinforcement of brittle matrices." *Journal of Physics D: Applied Physics* 4.11 (1971): 1737.

4. Stang, Henrik, and S. P. Shah. "Failure of fibre-reinforced composites by pull-out fracture." *Journal of Materials Science* 21.3 (1986): 953-957.

5. Mobasher, Barzin. *Mechanics of fiber and textile reinforced cement composites*. (9) CRC press, 2011.

6. Ma, Pibo, and Zhe Gao. "A review on the impact tension behaviors of textile structural composites." *Journal of Industrial Textiles* 44.4 (2015): 572-604.

7. Madhavi, Dr T. Ch, L. Swamy Raju, and Deepak Mathur. "Polypropylene Fiber Reinforced Concrete-A Review." *International Conference on Advances in Civil Engineering and Chemistry of Innovative Materials (ACECIM'14)*. 2014.

8. Zonsveld, J. J. "Properties and testing of concrete containing fibres other than steel." *RILEM Symposium on Fiber-Reinforced Cement Concrete, London*. 1975.

9. Hannant, D. J., J. J. Zonsveld, and D. C. Hughes. "Polypropylene film in cement based materials." *Composites* 9.2 (1978): 83-88.

10. Nagabhushanam, M., V. Ramakrishnan, and Gary Vondran. "Fatigue strength of fibrillated polypropylene fiber reinforced concretes." *Transportation Research Record* 1226 (1989): 36-47.

11. Bayasi, Ziad, and Jack Zeng. "Properties of polypropylene fiber reinforced concrete." *Materials Journal* 90.6 (1993): 605-610.

12. Fanella, David A., and Antoine E. Naaman. "Stress-strain properties of fiber reinforced mortar in compression." *Journal of The American Concrete Institute* 82.4 (1985): 475-483.

13. Stang, Henrik, Barzin Mobasher, and S. P. Shah. "Quantitative damage characterization in polypropylene fiber reinforced concrete." *Cement and Concrete Research* 20.4 (1990): 540-558.

14. Mobasher, Barzin, H. Stang, and S. P. Shah. "Microcracking in fiber reinforced concrete." *Cement and Concrete Research* 20.5 (1990): 665-676.

15. https://assets.master-builders-solutions.basf.com/Shared%20Documents/EB%20Construction%20Chemcials%20-%20US/Admixture%20Systems/Data%20Sheets/MasterFiber/basf-masterfiber-mac-2200-cb-tds.pdf

16. Mobasher, B., Li, C.Y., Modeling of stiffness degradation of the interfacial zone during fiber debonding, Composites Engineering 5 (1995) 1349-1365.

17. S. Igarashi, A., Bentur, S. Mindess, The effect of processing on the bond and interfaces in steel fiber reinforced cement composites, CemConcr Compos, 18 (1996) 313-322.

18. Reinhardt HW, Krüger M, Bentur A, Brameshuber W, Banholzer B, Curbach M, Jesse F, Mobasher B, Peled A, Schorn H. Textile Reinforced Concrete - State-of-the-Art Report of RILEM TC 201-TR, Ed. W. Brameshuber. 2006.

19. Sueki, Sachiko, et al. "Pullout-slip response of fabrics embedded in a cement paste matrix." Journal of Materials in Civil Engineering 19.9 (2007): 718-727.

20. Vincent J. Parks "Strain Measurement Using Grids", *Opt. Eng*. 21(4), 214633, Aug 01, 1982.

21. Chu, T.C., Ranson, W.F. & Sutton, M.A. Experimental Mechanics (1985) 25: 232. doi:10.1007/BF02325092

22. Yao, Y., et al. "Tension stiffening in textile-reinforced concrete under high speed tensile loads." Cement and Concrete Composites 64 (2015): 49-61.

23. Mobasher, B., Li, C.Y., Modeling of stiffness degradation of the interfacial zone during fiber debonding, Composites Engineering 5 (1995) 1349-1365.

24. S. Igarashi, A., Bentur, S. Mindess,, The effect of processing on the bond and interfaces in steel fiber reinforced cement composites, CemConcr Compos, 18 (1996) 313-322.

25. Reinhardt HW, Krüger M, Bentur A, Brameshuber W, Banholzer B, Curbach M, Jesse F, Mobasher B, Peled A, Schorn H. Textile Reinforced Concrete - State-of-the-Art Report of RILEM TC 201-TR, Ed. W. Brameshuber. 2006.

26. Sueki, Sachiko, et al. "Pullout-slip response of fabrics embedded in a cement paste matrix." Journal of Materials in Civil Engineering 19.9 (2007): 718-727.

27. Reinhardt HW, Naaman A.E. High Performance Fiber Reinforced Cement Composites 2-Proceedings of the second international RILEM -31, 172-1995

28. Peled, A., D. Yankelevsky, and A. Bentur. "Bonding and Interfacial Microstructure in Cementitious Matrices Reinforced by Woven Fabrics." MRS Proceedings. Vol. 370. Cambridge University Press, 1994.

29. Bartos, P. "Brittle matrix composites reinforced with bundles of fibres." Proceedings of the 1st Int. RILEM Congress from Materials Science to Construction Materials Engineering. Vol. 2. 1987.

30. Cohen, Zvi, and Alva Peled. "Controlled telescopic reinforcement system of fabric–cement composites—Durability concerns." Cement and Concrete Research 40.10 (2010): 1495-1506.